# IOSI PROJECT FINAL TECHNICAL REPORT

| | |
|---|---|
| Project Number | IOSI 2016-01 |
| Project Title | Laboratory investigation of transport, segregation and deposition of TSRU tailings in subaerial beach environments |
| Project Budget and Tenure | $181,825, April 19, 2017 to May 31, 2019 |
| Principal Investigator | Jeffrey D.G. Marr |
| Co-Investigators | Kimberley Hill |
| Highly-qualified personnel (HQP) | Rochelle Widmer, MS student |
| Industrial Stewards | Atoosa Zahabi (Imperial Oil)<br>Karsten Rudolf (CNRL)<br>Michael Graham (CNRL)<br>David Rennard (formerly with Imperial Oil) |
| Report Prepared by | Jeffrey DG Marr, Kimberly Hill, and Rochelle Widmer |
| Date | July 31, 2020 |

High-resolution file and figures are available and can be requested from IOSI (email semagina@ualberta.ca)

## DISCLAIMERS

Alberta Innovates (AI) and Her Majesty the Queen in right of Alberta make no warranty, express or implied, nor assume any legal liability or responsibility for the accuracy, completeness, or usefulness of any information contained in this publication, nor that use thereof infringe on privately owned rights. The views and opinions of the author expressed herein do not necessarily reflect those of AI or Her Majesty the Queen in right of Alberta. The directors, officers, employees, agents and consultants of AI and the Government of Alberta are exempted, excluded and absolved from all liability for damage or injury, howsoever caused, to any person in connection with or arising out of the use by that person for any purpose of this publication or its contents.

The University of Alberta makes no warranty, express or implied, nor assumes any legal liability or responsibility for the accuracy, completeness, or usefulness of any information contained in this publication, nor that use thereof infringes on privately owned rights. The views and opinions of the author expressed herein do not necessarily reflect those of the University of Alberta. The directors, officers, employees, agents, students and consultants of the University of Alberta are exempted, excluded and absolved from all liability for damage or injury, howsoever caused, to any person in connection with or arising out of the use by that person for any purpose of this publication or its contents.

## Executive Summary

Here we report on a series of laboratory experiments investigating the **transport**, **segregation**, and **deposition** of TSRU tailings in tailings ponds, e.g., external tailings facilities (ETFs). The motivation of the project was to develop insights into the unique processes that are associated with TSRU tailings and determine if there are opportunities to improve processes and outcomes of tailings storage in tailings ponds.

The experiments used field and operational data to design a specialized facility and hydraulic conditions that replicated full-scale hydraulic condition. The unit discharges (discharge per unit width) was estimated for the field and modeled in the lab. The 0.1 m wide by 10 m long flume represented the dynamics existing within a quasi-2D "slice" (or cross-section) of a fully 3D beach deposit. The experiment effectively simulated an active channel flowing over the beach and entering the pond environment. The clear walls of the flume provided opportunity to study the physics of transport, segregation, and deposition associated with TSRU tailings disposal.

The research involved two phases of study covering a range of different particle size distributions and included surrogate tailings materials (Phase 1) and real TSRU tailings (Phase 2). We also investigated effects of changing influent discharge and solids concentrations. The results between the TSRU tailings and surrogate tailings were qualitatively similar. With these similarities and the quantitative differences, the project reveals insight into parameters that influence effectiveness of particle capture on the beach of a tailings pond.

The experiments identified three regions or zones within the simulated tailings ponds with distinct transport, segregation and deposition processes. The figure below defines these three regions and below we summarize the salient transport, segregation, and deposition processes in each region.

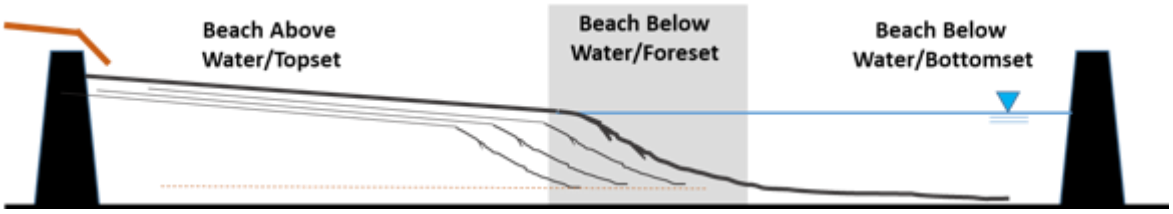


*I. Transport*

At a typical time in the beach build-out process, tailings are carried along with the fluid via several different processes, depending on their relative weight and sizes and the local slope. The typical transport modes are described below:

(1) The smallest and least dense particles move as a suspension in the fluid, that is, they move almost entirely like they are an integral part of the fluid. In other words, the smaller lighter particles move locally as essentially a single phase with the fluid.
(2) The larger and denser particles sink to the bottom of the flow and often have interactions with other particles and the bed. They are transported from this lower point in a way that depends on flow dynamics and local slope. For possible processes are described below:
    a. For conditions of vigorous flow and lower slopes, particles are transported downstream along the bottom boundary of the flow by the fluid in a moderately dense

sheared layer. This is often defined in the geology literature as "vigorous bedload conditions" or "bed sheet flows".

b. For conditions of gentle flow along low slopes, particles are transported downstream by the fluid under bedload and suspended load transport conditions.
c. For conditions of less vigorous flow and higher slopes, particles are carried primarily by their own weight in a high density layer that cascade or slides down the slope.
d. For conditions of vigorous flow and higher slopes, the particles are transported by a combination of gravity down the slope such as describe above (c) but may also be influenced by the flow field resulting in measurable downstream transport of coarse material.

As we describe in more detail in the body of the report, at any instant in time, most or all of these phases exist concurrently at different parts of the flume. For this summary, it is most useful to envision this in the context of steady state, after an initial deposit is built up.

*Transport in the Beach Above Water (BAW)*

After the particle-fluid flow (discharge) exited the pipe and passed through the plunge pool, it entered the BAW, characterized by a relatively low self-formed slope. The transport in this region was that of category (a) above. The smallest particles were contained in a narrow high-speed turbulent flow and the medium and larger particles moved along the bed in a multi-particle thick sheared flow.

*Transport in the BAW/BBW Transition*

At the downstream extend of the BAW, the slope of the deposit abruptly steepened into what is defined as the foreset. In this report we also refer to this location at the BAW/BBW Transition. As the flow entered the pond, it slowed relatively quickly, leading to a transition from category (a) to (d) to (c) in the categories above. The finest particles stayed in suspension, while medium and larger particles were increasingly carried down the slope by their own weight or, as will be discussed below, through particle avalanching and kinetic sieving processes.

*Transport in the Beach Below Water (BBW)*

The third and final stage of the transport consisted of a much gentler and slower average local velocity and low slope; transport of category (b) above. Once the flow reached the bottom or toe of the foreset, the slope became much lower. We observed two primary transport processes in this region. For experiments with significant fine or medium sized solids, such as Surrogate Mixture B and TSRU tailings, a sediment laden, sustained turbidity current formed and moved particles into the BBW region. At distances far from the foreset, the flow became nearly stationary. This region is the analog of the tailing ponds far from the BAW.

*II. Segregation*

In this section we describe the active *segregation dynamics*. That is, we summarize the observed physics of the segregation processes that dominated while the particles were flowing.

*Segregation in the BAW*

As the particle-fluid flow (influent) entered the BAW at the inlet there was a near-instantaneous segregation of the smaller less dense particles from the rest of the particles. The vigorous flow over the relatively low slope transported a range of the lighter particles in suspension. Only the heavier (larger and/or denser particles) fell to the bottom boundary and were transported as a sheared layer. In this sheared layer another segregation mechanism was evident, known as dynamic sieving.

Specifically, the smaller particles in the sheared layer find openings to drop toward the bottom of the layer, forcing the larger particles upward to the top of the sheared particle layer. The segregation dynamics observed in the BAW include:

- The top of the flow flowed at maximum velocity and carried lighter particles along with the flow and at a relatively low concentration.
- The bottom of the flow was sheared much more slowly and consisted of a relatively high concentration of larger particles. What is often called "Kinematic" or "Dynamic" sieving (in the granular physics literature) led to the largest of the coarse particles rising to the top of this shear layer and the smallest of the coarse particles sheared slower at the bottom.

*Segregation in the BAW/BBW Transition*

At the upstream extent of the foreset or transition region, the slope abruptly steepened and local flow depth increased resulting in a dramatic decrease in flow velocity. The segregation processes that dominated in this region were controlled by this transition from fast to slow velocity and also the concentrated near-bed shear flow that occurs in a gravity-driven dense particle flow. Specifically, as the local fluid velocity slowed, the intermediate sized particles rapidly fell out of suspension and drop into the shearing gravity-driven flow on the bed. This gravity-driven flow was dominated by "kinetic sieving", where the largest particles move toward the surface of the sheared gravity-driven particle layer, and the smaller large particles move away from this interface toward the deposit.

- The finest particles remained in suspension, though the average size in this suspension was finer than the BAW because of the slower velocities and thus lower "suspension dynamics". This material passed to the BBW.
- The shear region adjacent to the bed, somewhat thicker than the shear region on the BAW, had a wider range of particle sizes from the (smaller) particles that dropped out of the flow during kinetic sieving to the largest particles segregating at the top of foreset.
- The gravity-driven particle flow often (depending on the mixture and flow conditions) appeared to be episodic with failures occurring every 5-15 seconds.

*Segregation in the BBW*

Segregation within the BBW was primarily based on two transport processes. The first was the segregation associated with gravity current dynamics. Within the TSRU tailing experiments in particular and to some extent Surrogate Mixture B, a persistent gravity current or turbidity current formed along the bottom of the pond. The density contrast of this current and the surrounding pond water drove the flow down the foreset and onto the BBW deposit transporting solids to the end of the research flume. Solids settled out of this current resulting in a downstream fining. The second process was associated with particle settling out of nearly stationary flow occurring well away from beach or after the experiment was complete.

### *III. Deposition*

In this section, we relate the effects of the transport dynamics and active segregation dynamics on preferential deposition of specific particle sizes in the different regions of the deposit. It is important to state here that, while the transport and segregation discussion above consider the instantaneous process at work, the final deposit is an assemblage of many processes. The foreset and beach are continually prograding into the pond and as they do they build on top of BBW deposits. The full

thickness of the BAW deposit includes BBW deposit, BAW/BBW Transition processes and BAW processes.

*Deposition in the BAW*

In the BAW, the particle and fluid supply were held constant during an experiment. The bedload transport dynamics under these conditions forced the bed slope to adjust toward an equilibrium transport condition that was independent of influent flow rate. Once formed the BAW slope remained relatively throughout the experiment. Data from both surrogate and TSRU tailings experiments showed an inverse relationship between BAW slope and discharge. Average flow depth increased with influent discharge. The data suggests the BAW depth and slope self-adjusted to equilibrium bed shear stress that was unique to the specific tailings mixture being studied and inlet flow conditions.

In general, the deposition of material on the BAW topset was a small percentage of the total beach volume and this is attributed to the shallow slope of the beach. Furthermore, the particles added to the deposit in this region were limited to the particles at or near the bottom of the "bed sheet layer". The smallest of the larger particles were in suspension during the transport conditions, and the largest were moving at the top of the shear layer in this region. Thus, the particles that were deposited in this region (near the top of the deposit), represent the middle of the grain size distribution.

*Deposition in the BAW/BBW Transition*

At the foreset, particles dropped out of transport at a dramatic rate. For the surrogate tests, this region was responsible for the majority of the beach growth. It was also a major component of the TSRU tailings beach however TSRU tailings also had a substantial BBW deposit. In terms of grainsize, intermediate to smaller sized particles dropped out of suspension and then, through kinetic sieving, were quickly transported away from the surface of the gravity-driven shear layer. Thus, somewhat counter-intuitively, they deposit in the top and middle of this slope. The larger particles continue to the bottom and comprised most of the bottom of this layer.

*Deposition in the BBW*

The transport and segregation processes observed with the BBW included those associated with a sustained turbidity currents and particle settling. The turbidity currents had the effect of distributing coarser solids farther into the BBW. Surrogate Mix B (Tests 5 and 6) had a visible turbidity current and the BBW deposits were thicker than Surrogate Mixture A that had a very week turbidity current. The TRSU tailings experiments formed strong turbidity currents and developed thick BBW deposits downstream of the foreset. Grainsize analysis from these deposits showed the sand content within the BBW increased in concentration and distance into the pond with increasing discharge. Data also suggest high discharges yielded lower concentrations of fines in the deposit suggesting the fines were washed out of the flume during the experiments.

In experiments without a strong turbidity current or after the experiment was complete the deposit was formed primarily of the last solids to drop out of suspension, the finest particles. In reality, these also were transported farther and farther into the pond and in some cases out of the flume.

## Summary of findings specific to TSRU tailings

**TSRU tailings undergo segregation during deposition and appear to be influenced by parameters that presumably can be controlled by plant operation.**

1. Influent flow rate and composition of solids (grainsize and particles density) appear to influence the resulting BAW slope. For a given mixture, increases in flow rate result in a decrease in BAW slope.
2. The percentage of influent solids that contributes to the beach deposit decreased with increasing discharge and range from 83% at the lowest discharge to 65% at the highest.
3. Froth formation at the inlet, resulting from air entrainment at the plunge-pool/scour hole, appears to promote the segregation of bitumen and fines and the amount of fines segregation increased with discharge. The experiments data suggest that at higher discharge, more fines are removed as froth resulting in a lower concentration of solids (fines and sand) leaving flowing off the beach.
4. Froth islands formed over the channel and resulting in pressurized flow, scouring nearly complete bypass of solids to downstream of the froth.

**Distinct transport, segregation and deposition processes were observed in this study. Understanding the mechanistic involved in transport and deposition provide greater ability to optimize deposit characteristics and effectively operate tailings ponds.**

1. The grainsize distribution of tailings solids influences processes in BAW and BBW such as slopes, foreset height, thickness of BBW deposit, and formation of sustained turbidity currents offshore of the BAW.
2. BAW/BBW transition is a region of active deposition in a pond as is the BBW. Deposition on the topset of the BAW region was minor, comparatively.

**The project highlight the usefulness of controlled laboratory experiments to study field-scale process that are otherwise impossible to visualize and where tailings materials are challenging to work with.**

This project was funded by a grant from the Institute for Oil Sand Research (IOSI Grant 2016_01) and the Canada's Oil Sands Innovation Alliance (COSIA). In-kind resources were provided by the University of Minnesota.

## Table of Contents

## TABLE OF CONTENTS

## List of Figures

## List of tables

## Acknowledgment

The project team would like to thank COSIA Project Stewards for their support of this work. We appreciate the many hours of guidance, knowledge-sharing as well as technical and administrative support provided throughout the project. Our project Stewards included:

Atoosa Zehabi (Imperial Oil)
Karsten Rudolf (CNRL)
Michael Graham (CNRL)
David Rennard (formerly with Imperial Oil)

Special thanks to the student and staff at the St. Anthony Falls Laboratory for help with experiments and data collection reminding us that it takes many hands to complete a successful experiment. This includes: Ben Erickson, Aaron Ketchmark, Jim Tucker, Amirezza Ghasemi, and Eleanor Arpin.

This project was funded by a grant from the Institute for Oil Sand Research (IOSI Grant 2016_01) and the Canada's Oil Sands Innovation Alliance (COSIA). In-kind resources were provided by the University of Minnesota.

## Introduction

This final project report summarizes the experiments and findings of a large set of laboratory-based experiments focused on studying the transport and deposition of Tailings Solvent Recovery Unit (TSRU) tailings in external pond environments. The research was carried out at the University of Minnesota (UMN) over a two-year period of time and included two distinct phases of research. The first phase (Phase 1) examined transport and depositional processes associated with surrogate (simulated) tailings materials. The second phase (Phase 2) examined real TSRU tailings, which were provided to the UMN by an industry partner.

The experiments were carried out in a research flume specially designed for the project. The flume was 10 cm wide and 10 m long with clear walls to allow observation of the tailings transport and deposit formation. A detailed description of the experimental setup is provided in the sections below. The results of the Phase 1 and Phase 2 experiments provide important insights into the physical processes associated with the transport of fine-grained and coarse solids within the beach and pond environment and illustrate how transport mechanism are closely linked to segregation processes and character of the final deposit.

## Background

The surface mining and refinement of oil sands ore results in waste material (tailings) that contains natural clays, silts and sands, process chemical used to liberate bitumen, water, and low quality bitumen material (Beier, Wilson, Dunmola, & Sego, 2013). There are several types of tailings material generated during refinement and each has different properties related to particle sizes, water content, temperature, viscosity, solids content and so forth. Herein, the focus is on the tailings material produced from the tailings solvent recovery unit known as TSRU tailings and is characterized as fine-grained material composed of silt- and clay-sized sediment, asphaltenes (low quality bitumen) and water.

TSRU tailings are generated during the froth treatment process of oil extraction. During froth treatment, hydrocarbon chemicals, referred to as diluents, are added to the froth to promote further separation of solids, water, and asphaltines from the higher quality petroleum. Two general types of hydrocarbon chemicals are currently used with pros and cons of each. Based on the quality of the source ore, the froth characteristics, the desired final product characteristics, and operational/design decisions made by the facility, either naphthenic hydrocarbons or paraffinic hydrocarbons are used. The diluents are added to the froth causing the density and viscosity of the bitumen to lower allowing it to vertically separate from water and also allowing unwanted solids and low quality bitumen to settle vertically downward. This settled material is captured and further processed to remove water and strip off hydrocarbons. Typically, the material enters a Tailing Solvent Recovery Unit (TSRU), which heats the material to >100°C to “flash” clean the tails and recapture and recycle the solvents, which are then conveyed back into the processing plant. The waste product leaving the TSRU is TSRU tailings and is pumped to tailings ponds or other storage areas.

Each facility has unique processes for generating and disposing of TSRU tailings however in this study, we focus on storage of the TSRU tailings in tailing ponds, e.g., external tailings facilities (ETFs). Tailings ponds are large surface ponds designed to capture tailings materials and process water and they also serve to clarify process water so it can be recycled back through the processing plant. The TSRU tailings enter the tailings pond through large open-ended pipe(s) that discharges subaerially into the pond. The tailings material is pumped through the pipe as a high temperature, well-mixed slurry of solids, bitumen and water with solids content ranging from 10 to 25%wt. (D. Rennard,

personal communications). The tailings slurry enters the relatively quiescent pond and segregation of the solid, bitumen and the water immediately begins.

TSRU tailings are unique from other tailings streams in that the solids (non-bitumen material) are fine grained with a majority of the solids <200 microns. The bitumen present in the material is also predominantly composed of asphaltines, which are low quality bitumen intentionally removed from the final refined product. The fine-grained solids, asphaltines, and the temperature-dependent nature of the bitumen contribute to complex behaviors of the TSRU tailings as they are placed in the tailings pond environment. A summary of these complexities is provided below:

- The fine-grained nature of the solid fraction of TSRU tailings, which does include some sand but mostly particles sizes <44 micron, results in slow settling rates of particles and thus lower sloped surfaces in the tailings pond. A concern with all tailings input into tailings pondss is the loss of fine particles (fines) to the pond or, in other words, inability to capture the fines within the beach deposit. TSRU tailings deposits are also slow to dewater and remain "fluidized" for long periods of time.
- The asphaltines in the TSRU tailings are thought to aggregate together forming a*sphaltine aggregates*. Aggregates are conglomeration of asphaltines that hold on to additional water and fine solids within their structure. There is some thought that they help to capture fines in the aggregate but if aggregates break up or are sheared during transport and deposition, they can release fines into the pond. The additional water held in asphaltine aggregates are also thought to slow down dewatering process of the deposit.
- Temperature is another important factor in TSRU tailings. While not studied in this project, TSRU tailings are discharged at >90°C and cool as they move into the tailings pond environment. The rheologic properties of the bitumen change dramatically with temperature and it is hypothesized that transport and depositional processes may also change.

## Project Motivation

TSRU tailings are a unique tailings stream characterized by high fines and water content and asphaltine aggregates. The presence of the aggregates as well as their role in how solids are transported and deposited is important for planning and operation of the tailings pond with implications for fines capture in the BAW and impact on fines delivery into the pond.

As described above, TSRU tailings are produced by the bitumen extraction process during froth treatment (Xu et. al, 2013). The Oil Sands industry is under growing pressure to improve or eliminate the need for storage of tailings in tailings ponds (Xu et. al, 2013). Additionally, there is greater public pressure, through regulation, for quicker treatment of process water and reduction in the volume of tailings produced by mines (IOSI, 2015). Finally, emphasis is focused on lowering the concentration of fines tailings that reach the pond through greater capture of fines in the subaerial beach.

## Project Objectives

The project has the following objectives:

- Develop a robust facility and testing protocol for examining transport and depositional behavior of TSRU tailings under simulated field scale conditions.
- Through the observations and findings of the experimental program, develop insights on the following questions:
    - How does the TSRU tailings beach slope change as a function of the input discharge?

- How will degree of segregation of the TSRU tailings in the final deposit change as a function of mixture properties and inflow rate?
- How do the asphaltine aggregates alter the transport and depositional behavior from a typical coarse/non-cohesive tailings stream?
- How is fines capture within the TSRU tailings deposit linked to input flow rate and local transport/depositional conditions?

We note that deeper investigations related to asphaltine aggregates were beyond the refined scope agreed upon with the project stewards, specifically regarding the agglomeration and break down of asphaltine aggregates. If time in a future project allows, we recommend considering the following related questions that likely influence the above results:

- Under what conditions do asphaltine aggregates break down through the action of bed shear stress or other conditions?
- Are there conditions where asphaltine aggregates grow or conglomerate in the flow?

## Overview of Experimental Program

The project involved two phases of laboratory experiments and both used the same facility and data acquisition setup. Phase 1 was a series of experiments using surrogate TSRU tailing mixtures. The surrogates were mixtures of commonly available solids (clay, silts, and sands) that matched grainsize and settling properties of TSRU tailings. Phase 2 was a series of experiments that utilized real TSRU tailings.

The experimental approach and data collection methods were the same for both phases of experiments. In the next section, we describe the Experimental Design and the Data Collection Design used in this project. Following these sections, we provide detailed summaries of both Phase 1 and Phase 2.

## Experimental Design

*Field hydraulic conditions*

Figure 1 is an aerial image taken above a TSRU tailings beach on a typical operational day. From the image, it is possible to observe a few key characteristics of the deposition environment:

1) The TSRU tailings enters the pond through a point source (end of pipe) discharge point and the beach deposit forms radially outward from this location.
2) The beach surface is formed by "fluvial-braiding". The influent TSRU tailings stream quickly transitions from a single point location to many active channel that have a braided fluvial morphology and flow away from the point source. We know from observations of braided depositional fans that these channels are continually moving and changing positions. Over time they rework the entire fan surface creating the radial deposit or beach.
3) There is a distinct shoreline position where the deposit transitions from Beach Above Water to Beach Below Water. Again, from observations of alluvial fans, and assuming the pond elevation does not change over time, we know that this shoreline position advances outward, away from the source, into the pond.

**Figure 1. Aerial image taken over a TSRU tailings beach formed in an external tailings facility.**

To experimentally simulate the processes described above, we adopted a design approach that sought to replicate full-scale channel hydraulics and influent discharge rates as observed in the field. To help in this design effort, Project Stewards provided the research team with field data from an active TSRU tailings basin. Images were provided along with operational conditions at the time of the image. Table 1 summarizes the data received. The data included the total discharge of TSRU tailings into the pond, $Q_w$, and the density of material.

**Table 1. Summary of example operational conditions containing the flow rates and density readings for TSRU tailings pond on various days between July 19, 2014 and February 17, 2017.**

| Date | Discharge ($m^3$/hr) | Density (kg/$m^3$) | Second Flow Rate ($m^3$/hr) | Second Density (kg/$m^3$) |
|---|---|---|---|---|
| **July 19, 2014** | 2600 | 1000 | - | - |
| **March 30, 2015** | 2500 | 1000 | - | - |
| **July 29, 2015** | 2500 | 1040 | 4000 | 1000 |
| **September 9, 2015** | 2200 | 1020 | 3500 | 1000 |
| **May 5, 2016** | 3000 | 1000 | 1950 | 1000 |
| **September 22, 2016** | 0 | 1600 | 2500 | 1040 |
| **February 17, 2017** | 2150 | 1000 | 2200 | 1150 |

Using the total discharge data at the source (column labelled "Discharge") along with the corresponding image from the same date, the research team estimated the approximate hydraulic conditions occurring on the fan surface. The unit discharge was used as the primary flow characteristic and was determined using the following approach.

1. Aerial images of the fan and corresponding operational conditions were selected.
2. Images were scaled to real-world dimension using ground targets identified in the image.
3. The point-source discharge location was identified in each image and defined as a radial flow boundary.

4. Using CAD Software, a radial distance was selected and added to the photograph (Figure 2).
5. The radial flow boundary was segmented into 18 different segments at 20° each. The arc length was determined, $l_R$.
6. By carefully studying the photographs, the research team estimated the percentage of each segment that contained "active" flow crossing the radial boundary. This percentage of active flow was multiplied by $L_R$ to determine the wetted length within that segment, $L_{RW}$.
7. Repeating this process for all 18 segments and summing together the wetted lengths for each segment, the research team estimated the total wetted length at a radius from the source.
8. Assuming that flow volume was conserved, the total influent discharge was divided by the wetted length yielding a unit discharge, $q_w$, where

$$q_w = \frac{Q_{w,\ influent}}{L_{w.total}} \qquad \text{(units of m}^3\text{/s-m)}$$

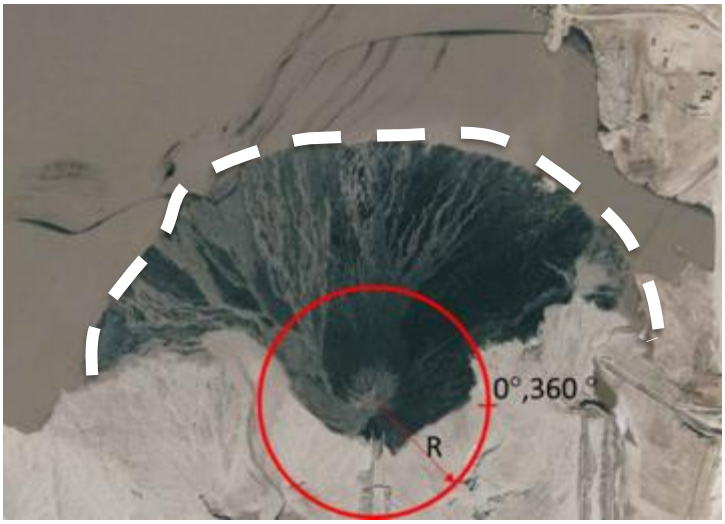


**Figure 2. Example of scaled image analysis to determine unit discharge. The white dashed line indicates the approximate location between the beach above water (BAW, where the top of the sediment deposit is above the pond surface) and the beach below water (BBW, where the top of the sediment deposit is below the pond surface).**

This procedure was repeated at three different radii, 50-m, 90-m, and 125-m for the six different references conditions (i.e. photo and operational data on a single day). Table 2 summarize the minimum, average, and maximum unit discharge estimated from this evaluation.

**Table 2. Summary of estimated unit discharge, $q_w$, for a typical TSRU tailings beach at three different radii.**

| | Radius: 50 m | | | Radius: 90 m | | | Radius: 125 m | | |
|---|---|---|---|---|---|---|---|---|---|
| Date | Min | Average | Max | Min | Average | Max | Min | Average | Max |
| July 29, 2014 | 5.2 | 6.0 | 6.3 | 2.3 | 4.2 | 6.1 | 1.7 | 2.8 | 4.1 |
| March 21, 2015 | 6.6 | 7.2 | 7.3 | 3.7 | 3.7 | 3.7 | 3.2 | 3.2 | 3.2 |
| September 9, 2015 | 13.0 | 13.9 | 14.1 | 0.4 | 5.8 | 11.8 | 0.7 | 6.7 | 14.5 |
| September 30, 2015 | 3.4 | 7.6 | 15.9 | 0.5 | 3.6 | 10.1 | 1.8 | 3.3 | 9.1 |
| May 5, 2016 | 7.9 | 9.9 | 13.1 | 4.4 | 7.3 | 8.8 | 0.6 | 2.3 | 6.3 |
| September 22, 2016 | 1.0 | 2.3 | 4.0 | 0.6 | 1.3 | 2.2 | 0.2 | 1.0 | 2.1 |

*Units: Unit discharge units are liters/second-meter*

Taking a step back, the values computed in Table 2 represent the average unit tailing flow rate that occurs within an active channel on the beach surface. We acknowledge that these channels are ever-changing in location, local slope, and channel cross-sectional profile however, for the purposes of exploring full-scale transport-deposition conditions, the analysis allows us to approximate local hydraulic conditions and use this information to design a research experiments, in particular the research flume that can approximate these conditions.

### *Flume design*

A new flume was constructed for these experiments. The flume width was set at 0.1 m with a wall height of 0.5 m and a total length of 10 m. The flume was constructed with clear acrylic walls and flat aluminum bed (Figure 3). A photograph of the flume is shown in Figure 4.

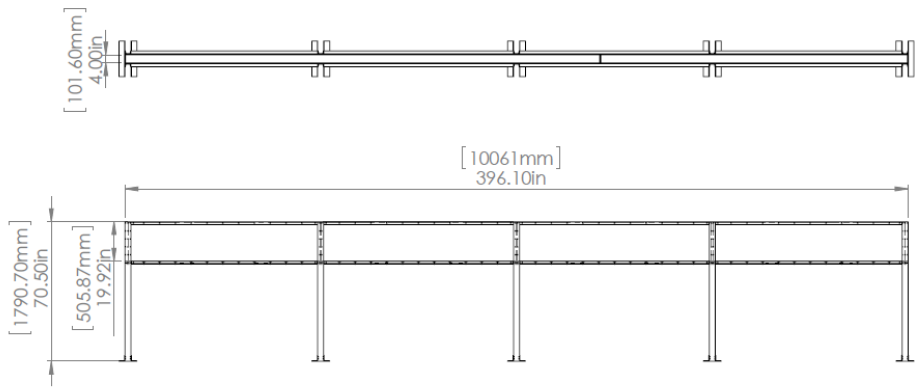


**Figure 3. Plan and profile view of research flume constructed for TSRU tailings research. The walls off the flume were constructed of clear acrylic. The framing and structural supports were fabricated from aluminum.**

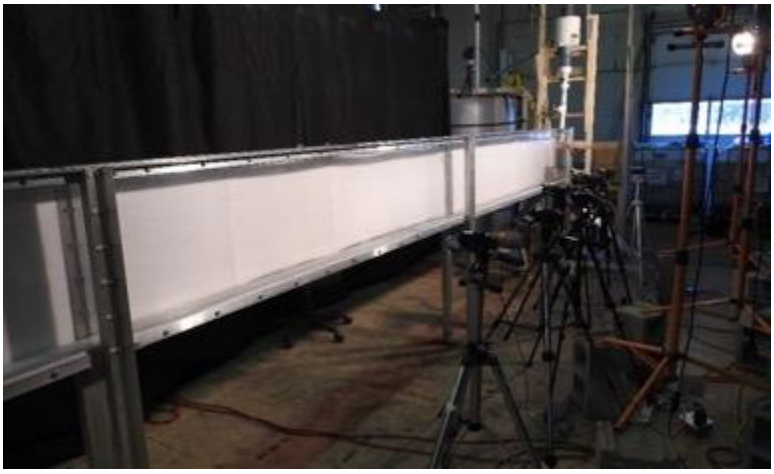

**Figure 4. Image of the upstream section of the research flume.**

### *TSRU tailings influent rate*

The range of unit discharge estimated from the field conditions along with the flume width selected for the research flume were used to determine the range of absolute discharge for the experiments. Unit discharge estimated for the field, $q_w$, multiplied by flume width yielded the discharge range for the experiments.

Table 3 is a summary of the average unit discharge estimated for each of the three radii evaluated via image analysis. Assuming a 0.1m wide flume, the range of absolute discharge is from 0.3 to 0.8 liters/second. Using these values, we designed a tailings slurry delivery system including mixing tank, pump, head tank and flow control valves capable of influent discharges ranging from 0.25 to 1.0 liters per second.

**Table 3. Summary of average unit discharge estimated from the field and equivalent absolute discharge used in the flume design.**

| Parameter | Radius: 50 m | Radius: 90 m | Radius: 125 m | Units |
|---|---|---|---|---|
| Unit discharge | 7.8 | 4.3 | 3.2 | liters/s-m |
| Absolute discharge assuming 0.1m width channel | 0.8 | 0.4 | 0.3 | liters/s |

### *Slurry mixing and delivery system*

In addition to the flume, the set-up included several additional pieces of equipment and these items are summarizes here.

**Storage and mixing tank:** A large, cubic meter-sized tank (i.e. tote) was used to hold the tailings materials prior to their discharge into the flume (Figure 5). The tote included a 6-inch port on the top through which a large mixer was inserted into the mixture. A 2-inch port located on the side wall of the tote was used to withdraw material from the tote. The tote was used as a mixing tank during the Phase 1 surrogate runs but was abandoned in the TSRU runs. This is explained more fully below.

To mix the materials before we pumped them into the flume, we used an industrial-sized mixer in our mixing tank. A Variable Frequency Drive (VFD) was wired to the mixer motor and allowed control over the speed of the mixer.

**Figure 5. Image of 1 cubic meter tote used to store and mix tailings material (surrogate test).**

**Pump and tailings delivery system:** A pump was used to deliver the tailings mixtures from the mixing tank to the flume. For the surrogate experiments, a pneumatic diaphragm pump was used and in the TSRU tailings experiments this pump was replaced with a centrifugal pump. The pump was connected to the tote through several feet of flexible hose. PVC pipe was used to convey tailings from the discharge side of the pump to a constant head tank located at the upstream end of the flume.

**Constant head tank:** Because the volumetric discharge delivered by a pump is determined by the hydraulic head upstream and downstream of the pump, as the level in the mixing/supply tote drops during the experiment, the pump discharge also changes. A constant head tank was used to ameliorate this. The constant head tank was fabricated from clear PVC so that the fluid level within the tank could be observed easily. The discharge line of the pump was routed through an adjustable gate valve and terminated just above the constant head tank, discharging into the free surface of the constant head tank. The operator adjusted the gate valve to maintain a constant free-surface elevation within the constant head tank over the duration of the experiment (Figure 6).

Tailings slurry flowed out of the constant head tank into the upstream end of the research flume. The influent discharge into the flume was set by a pre-calibrated orifice placed over the exit pipe of the constant head tank. PVC end caps were used for this. Using water as the fluid, the research team developed end-cap orifices with various opening sizes that yielded a range of discharges (0.25, 0.5 1.0 liters per second). The appropriate orifice was placed on the exit pipe of the constant head tank prior to the start of the experiment. After passing through the orifice, the mixture freely entered the flume. An image of the constant head tank used in the project is shown in Figure 7.

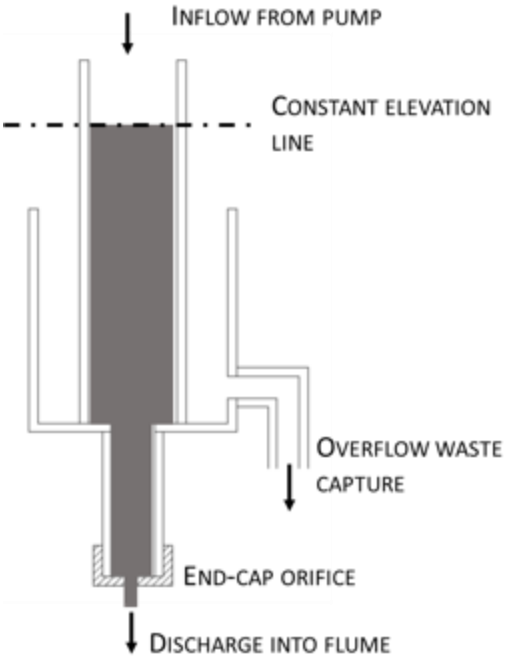


**Figure 6. Schematic of the constant head tank showing inflow and outflow as well as constant elevation line. The inflow from the pump was adjusted manually to maintain a constant free-surface elevation. This elevation was marked on the outside of the head tank and can be seen as a dark black band in Figure 7.**

**Figure 7. Image of the constant head tank.**

The final component of the tailings delivery system was a small stilling basin configured in the research flume. A 15-cm submerged wall was inserted into the flume 40 cm downstream from the upstream extent of the flume (Figure 8). Tailings mixture entered the flume as a jet at the upstream end of the stilling basin.

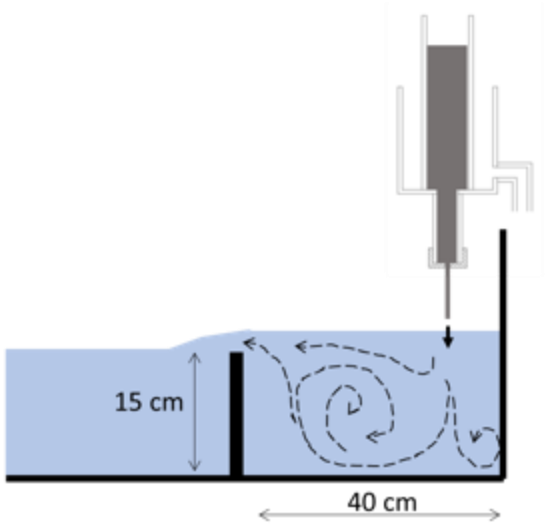


**Figure 8. Schematic of the stilling basin feature added to the first 40 cm of the flume. The stilling basin served to dissipate some of the inflow energy of the inlet and provided entrance conditions that replicate the plunge pool inlet condition existing in the field.**

## Data Collection Design

The following data collection systems and approaches were used during the project to capture transport, segregation, and deposition processes. Because these processes for TSRU tailing are impossible to observe in the field, our effort to replicate and observe these processes in a laboratory setting provides useful insights into the formation of tailings beaches.

### *Discharge measurements*

Influent flow rate was recorded using a sharp-crested weir and point gauge measurement located at the end the end of the flume (Figure 9). Depth of flow over the weir was recorded three to four times during each experiment. Because there is no water storage in the flume, the discharge measured at the exit of the flume (effluent) is equal to the influent volumetric flow rate of tailings (influent).

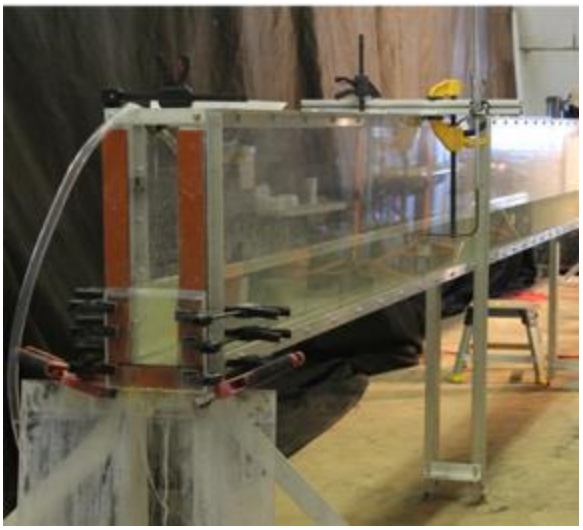

**Figure 9. Image of end plate on flume that was used to establish a 15-cm water depth in the flume. The end-plate also had a beveled top edge and served as a sharp-crested weir for discharge measurements. A manually operated point gauge was used to measure water surface prior to and during an experiment.**

### *Video cameras*

High definition digital video cameras were used to capture the transport of tailings, segregation of solids, and formation of the deposit (Figure 10). The cameras recorded in progressive frame mode at 60 frames per second. We focused each of the cameras on the inside surface of the flume and set cameras to manual focus. A metric tape fixed to the front face of the flume was within the field of view of each camera. The total field of view width was 60-cm for each camera.

**Figure 10. Image of the flume setup showing video cameras and lighting immediately prior to the start of a TSRU tailings experiment.**

### *Deposit surface tracking*

The deposit formed during an experiment evolved quickly over time. In order to track the evolution of this deposit, the research team recorded the position of the deposit surface by quickly drawing a contour line on the outer surface of the flume window (Figure 11). Colored dry-erase or grease pencils were used to draw the lines. After the completion of the experiment, these lines were surveyed and station/elevation data were recorded. These data are referred to as *deposit surface tracking.*

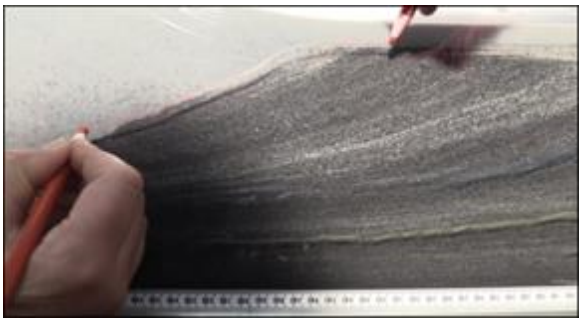

**Figure 11. Image showing method used for surface tracking.**

### *Suspended sediment sampling*

Suspended sediment samples were captured during the experiments using a grab sample technique with 125 ml containers. Samples were collected in a number of locations as follows:

- Mixing tank/tote samples - Samples pulled from the mixing tank prior to entering the flume.
- Influent samples – Samples collected at the outlet of the constant head tank, immediately before entering the flume.
- Shoreline grab samples – Samples collected ~15-cm downstream of the beach shoreline. This position was continually changing over the experiment. The research team identified this location and then captured the sample. The sample was captured from the top 3-4 cm of surface flow.

*Still photographs of final deposit*

The final deposit was recorded with still photographs using high quality digital camera on a tripod.

*Final surface elevation survey*

A point gauge was used to accurately measure the surface of the final deposit over the entire length of the flume.

*Deposit coring and analysis*

Following the completion of each experiments nine vertical sediment cores where taken from the deposit. Coring tubes were made from 2.6 cm diameter copper pipe cut to 33-cm lengths. The cores were sampled over the full-length of the deposit and specific positions were selected to capture both BAW, BBW deposits. The cores were removed from the flume and stored in a frozen state until ready for analysis. The processing of cores involved extracting the frozen material from the core tube and then subsampling the deposit into a top, middle and bottom sample. The position of this subsample divisions where made based on visual changes in the deposit and attempt to align the top sample with the topset, middle sample with foreset and bottom sample with bottom set. These samples were analyzed for particle size distribution using a Horiba LA-920 laser diffraction machine.

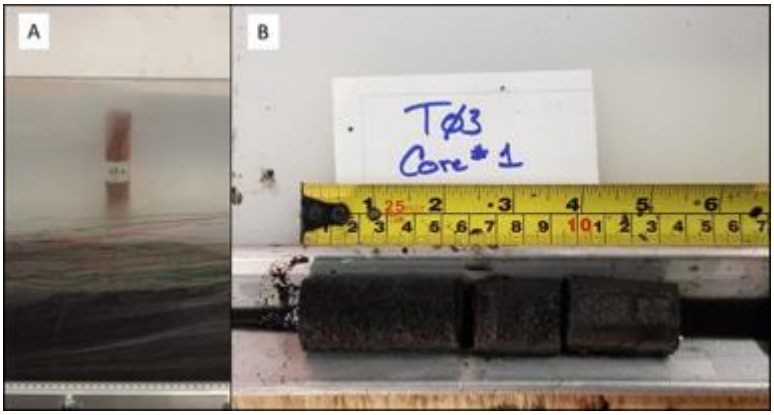


**Figure 12. (A) Image of a core tube placed into a deposit. (B) Extracted and subsampled core.**

# PHASE 1: SURROGATE EXPERIMENTS

## Overview

Prior to working with the TSRU tailings material and, in part, while the shipment details of the TSRU tailings material were being worked out, the research team carried out very informative experiments using simulated TSRU tailings. We refer to the mixtures studied here as "surrogate tailings". The composition of the surrogates were designed to replicate, as near as possible, the segregation behavior of TSRU tailings samples and used natural material (i.e. clay, coal, and sand) - non-hazardous and readily available components. The surrogate experiments also allowed the team to finalize the research procedures and data collection techniques necessary for the TSRU tailings experiments. In this section of the report, we summarize this first phase of research and the relevant results.

## Surrogate material

For the purpose of creating a surrogate mixture that behaved comparably to actual TSRU tailings, we conducted several bench top experiments on TSRU tailings samples received at the outset of the project. First, we estimated the volumetric concentrations of solids and process water in a 1.0 liter sample of TSRU tailings. We then observed the settling behavior of TSRU tailings to compare to other mixtures. The unique settling behaviors led us to test combinations of readily available materials.

### *TSRU tailings characterization*

Four liters of High Temperature (HT) TSRU tailings material were provide to the research team and the particle sizes, concentrations and settling characteristics were used to develop surrogate tailings mixtures. We determined the following properties for the TSRU samples:

**Table 4. Summary of basic TSRU tailings properties**

| Material Property | Value |
|---|---|
| Relative Density | 1 - 1.5 grams/cm^3 |
| Density (at 15.5 ºC) | 900 kg/m3 - 1200 kg/m^3 |
| Viscosity | 21 cSt (21 mm^2/s) at 40 ºC |
| Solids content (%wt including bitumen) | 14% |
| Water content (%wt including bitumen) | 86% |

The particle settling and segregation behavior of real TSRU tailings in a quiescent column was the primary characterization used to develop the surrogate. These observations were made in a 1 Liter graduated cylinder containing the TSRU tailing material. The column was capped with a stopper and then turned end-over-end to form a fully suspended mixture. The column was placed on a table and allowed to settle. A digital video camera documented the settling process. w Figure 13 shows the time-lapse images from one of the column settling tests. In addition to the video documentation of settling, we also recorded the position of the coarse layer (black) interface over time and used this information in developing surrogates (see Figures 14 and 15 below).

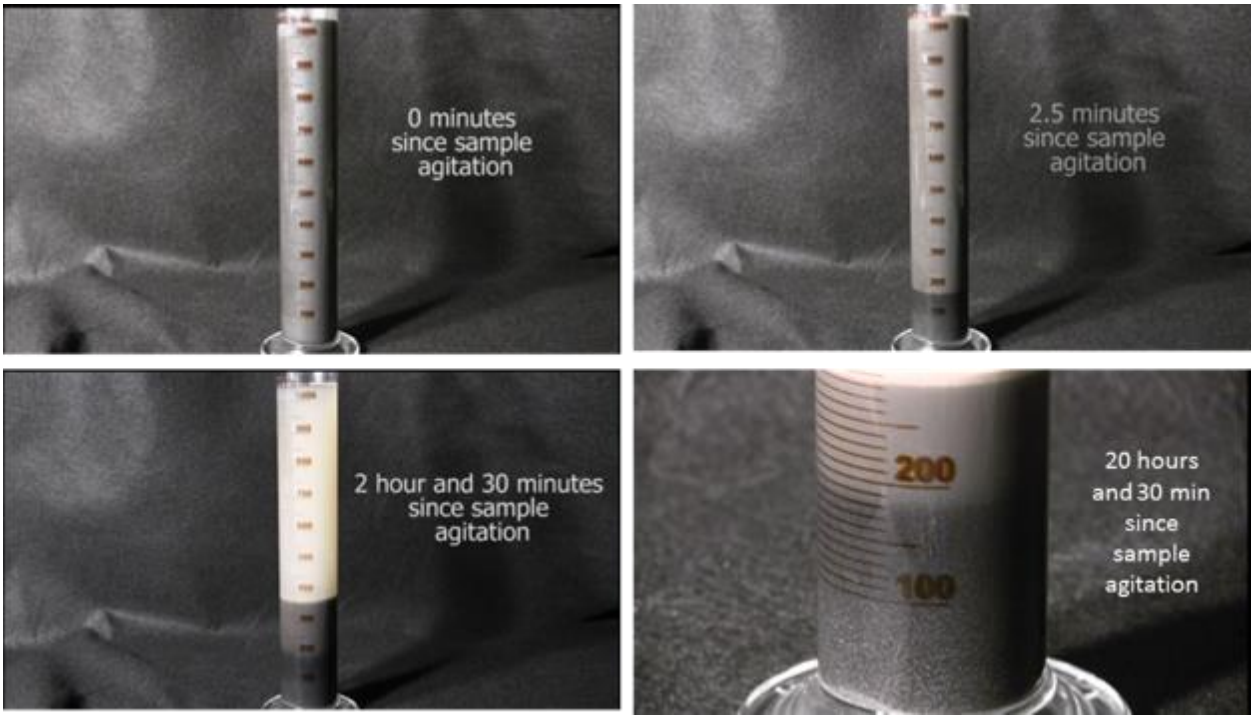


**Figure 13. Time-lapse images a settling test using TSRU tailings.**

The tailings formed two distinct sediment layers: one of dark colored - large particles that settled within a few minutes; and one of lighter colored - fine particles that took approximately one day to settle.

Careful inspection of the bottom dark layer showed that white particles (fines) appeared to be "trapped" within the matrix of the coarser particles. It also appeared visually that the concentration of fines was greater near the bottom of the black layer with decreasing concentration higher up in the layer. This observation suggests that the capture of fines may be linked to the rate of deposition of coarser material, i.e. rapid fallout of particles may be more effective in trapping fines than at slower settling rates. The lighter fine layer formed on top of the coarse black layer over several hours resulting in clarified cap water over the solids.

### *Surrogate development*

Two surrogate TSRU tailings slurries were developed using accessible and safe materials. The materials were mixed with tap water at similar solids concentrations to TSRU tailings. The materials tested included fine-grained ballotini (crushed and sieve glass), fine-grained sand, nepheline syenite, anthracite coal, and kaolinite clay.

#### *Surrogate A: Kaolinite and anthracite*

Surrogate A was a mixture of 6.5%wt anthracite coal and 1.5%wt kaolinite clay (The Cary Company, Snobrite Kaolin) and 92.1%wt. tap water. Total solids concentration was 8%wt. solids (Table 5). This mixture was simple with only two components but provide excellent visual difference between the two solids components. The anthracite was dark black and kaolinite was white or light grey in color. The mixture strongly displayed two-layer settling behavior similar to TSRU tailings. Details on the anthracite and kaolinite material as well as mixture characterizations is provided in Appendix C.

**Table 5. Summary of Surrogate A composition.**

| Component | %wt. | Density (g/cc) |
|---|---|---|
| Anthracite | 6.5% | 1.50 |
| Kaolinite | 1.5% | 2.82 |
| Tap water | 92.1% | 1.00 |

Settling behavior of Surrogate A was evaluated and compared to the TSRU tailing (Figure 14). Surrogate A coarse material (anthracite) settled faster than the coarse material within the TSRU tailings. We note the solids content of the surrogate was about half of the TSRU tailings (8%wt for surrogate versus 14%wt TSRU tailings).

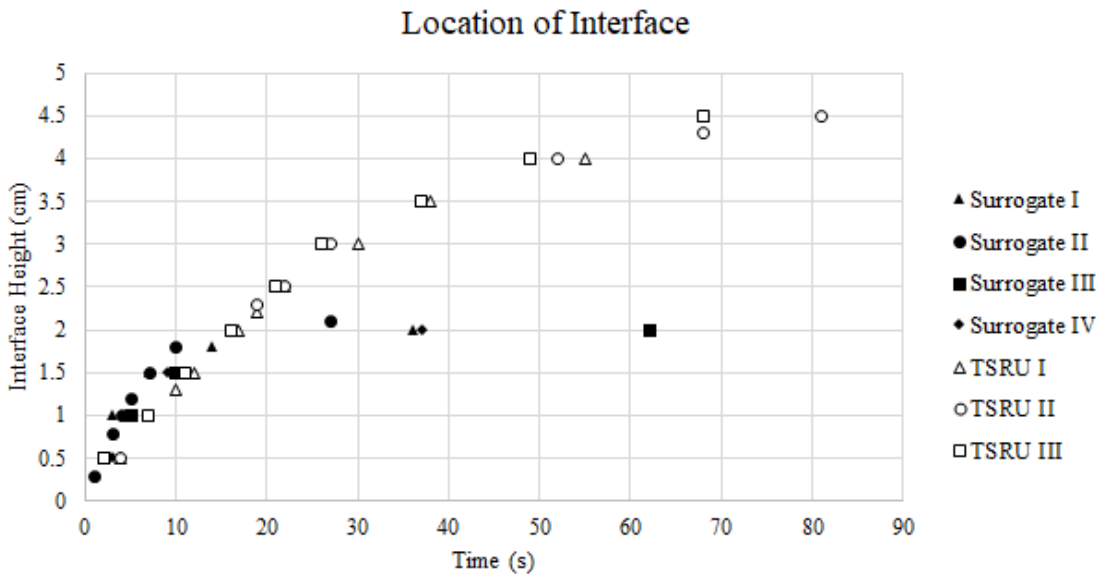


**Figure 14. Comparison of the coarse material settling interface over time for TSRU tailings and Surrogate A. Surrogate I-V and TSRU I-III indicates the various trials used for analysis; mixture compositions were not varied.**

## *Surrogate B: Kaolinite, anthracite and fine sand*

A second surrogate was developed and studied. Again, kaolinite clay and anthracite were used however a fine sand component was added (US Silica, F-80 sand). Total solids content was 10.5% wt. The fine sand was whole grain, pure white in color with a grainsize range of 60-500 micron and a median grainsize of 150 micron.

**Table 6. Summary of Surrogate B composition.**

| Component | %wt. | Density (g/cc) |
|---|---|---|
| Anthracite | 3.2% | 1.50 |
| Kaolinite | 1.4% | 2.82 |
| Fine sand | 5.9% | 2.77 |
| Tap water | 89.5% | 1.00 |

The settling behavior of the coarse material in Surrogate B was evaluated and compared with the TSRU tailings (Figure 15). The data match the TSRU tailings better both in rate of settling and total depth of coarse settled layer.

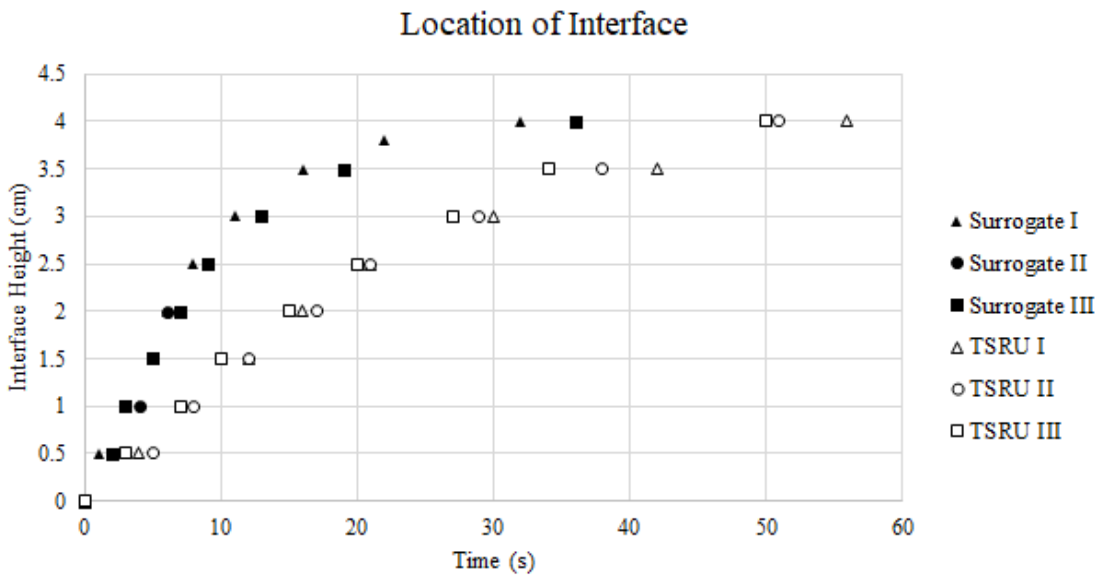


**Figure 15. Results from tracking the surface of the initially settled coarse layer of particles in both the TSRU tailings samples and the coal, clay, and silica surrogate mixture. Surrogate I-III and TSRU I-III indicates the various trials used for analysis; mixture compositions were not varied.**

## Test Matrix

Phase 1 involved flume experiments using the two surrogate mixtures (A and B) and using the facility set-up and data collection previously discussed. Table 7 is a matrix of the experiments performed with additional information on the flow rates and experiment duration.

**Table 7. Summary of Phase 1 experiments presented in this report.**

| Variable | Surrogate Test 2 | Surrogate Test 3 | Surrogate Test 5 | Surrogate Test 6 |
|---|---|---|---|---|
| Discharge (Target), L/s | 0.5 | 1.0 | 1.0 | 0.5 |
| Discharge (Actual), L/s | 0.5 | 1.0 | 0.9 | 0.6 |
| Surrogate mixtures | Surrogate A | Surrogate A | Surrogate B | Surrogate B |
| **Mixture (% vol. / % mass)** | **% vol. / % mass** | **% vol. / % mass** | **% vol. / % mass** | **% vol. / % mass** |
| Coal (anthracite) | 4.5% / 6.5% | 4.5% / 6.5% | 2.3% / 3.2% | 2.3% / 3.3% |
| Clay (Kaolinite) | 0.5% / 1.5% | 0.5% / 1.5% | 0.5% / 1.4% | 0.5% / 1.5% |
| Sand (110 micron) | - | - | 2.3% / 5.9% | 2.3% / 6.0% |
| Water | 95.0% / 92.1% | 95.0% / 92.1% | 95.0% / 89.5% | 95.0% / 89.5% |
| Volume Concentration | 5.0% | 5.0% | 5.0% | 5.0% |
| Solids Content (%wt) | 7.9% | 7.9% | 10.5% | 10.5% |

## Summary of Data Collection and Sampling

The data collection program employed in Phase 1 was detailed above but summarize again here.

- Discharge measurement
- HD video cameras

- Deposit surface tracking
- Suspended sediment sampling
- Still photographs
- Final surface elevation survey
- Deposit coring and analysis

## Results

### *Flow discharge, durations and volume/mass added.*

Table 8 summarizes the four tests reported here for surrogate experiments. As mentioned above, two surrogate mixtures were examined, each with a flow rate of ~0.5 l/s and ~1.0 l/s. The total mass of material input into the flume environment is also estimate and provided in the table.

**Table 8. Summary of experimental parameters for the four surrogate experiments.**

| Experiment | Average Discharge (Liters/second) | Duration (Minutes) | Total Volume (Liters) | Equivalent Unit Discharge (l/s-m) | Estimated Bulk Density (kg/m^3) | Total Mass Added (solids+water) (kg) | Solids content at Inlet (%wt) | Total Mass Added (solids) (kg) |
|---|---|---|---|---|---|---|---|---|
| Surrogate Test 2 | 0.56 | 22.0 | 739 | 5.6 | 1032 | 763 | 7.9% | 60.3 |
| Surrogate Test 3 | 1.04 | 13.3 | 830 | 10.4 | 1032 | 856 | 7.9% | 67.7 |
| Surrogate Test 5 | 0.93 | 14.0 | 781 | 9.3 | 1061 | 829 | 10.5% | 87.0 |
| Surrogate Test 6 | 0.59 | 25.5 | 903 | 5.9 | 1061 | 958 | 10.5% | 100.6 |

### *Observation of transport processes*

The deposits formed during Surrogate Test 2 and Surrogate Test 3 had three basic formation stages: the "initial stage" when the BAW deposit began to form, the "steady state" stage when the front did not change in shape but merely prograded downstream, and the "post-experiment" stage when the tailings delivery was completed and suspended particles were allowed to settle. We present our observations for these three stages.

#### *Initial Stage: Establishing Beach Above Water*

The initial condition in all experiments was an empty "pond" with a fixed depth of 15 cm. Tailings slurry was introduced at the upstream end as a point source and simulated an open pipe with a constant volumetric flow rate and approximately constant solids concentration. Upon entering the quiescent pond water in the flume, the energy of the tailings slurry quickly dissipated resulting in rapid deposition of the solids. For all four experiment, we observed a mound forming and growing vertically, and, at a slower rate, in the streamwise direction as well.

As the deposit grew in elevation to the point that the deposit surface approached the pond water surface, we observed a substantial change in process. First, the vertical growth slowed and second, the flow velocity of the incoming tailings stream became great enough that large coarse particles could no longer settle but were advected with the flow, much like a stream or channel environment. Here, we observe the initial formation of the BAW deposit. From this time forward, the beach construction became clear with sediment carried across the deposition surface toward the end of the beach – the BAW/BBW transition. Borrowing terminology used in geomorphology, the BAW is a delta and the upper surface of the deposit is the topset. The BAW/BBW transition is referred to as the

foreset, and the BBW deposit is referred to as the bottom set. An illustration of these processes is shown Figure 16.

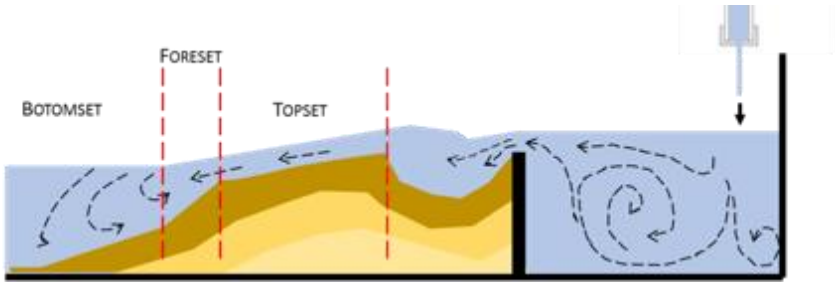


**Figure 16. Schematic of the deposit evolution leading to the formation of the BAW deposit. The various colors (cream, tan, and brown) are meant to represent the deposit at various times from the start of tailings feed (top) to after the time at which the plunge pool had reached a statistically steady state, nearly filled with sediment.**

The fine solids entering the basin were not captured at any significant rate in the BAW deposit and, in all four experiments, formed an initial turbidity current that traveled along the bottom until reaching the end of the flume. Figure 17 shows an image of the turbidity current taken from Surrogate Test 2.

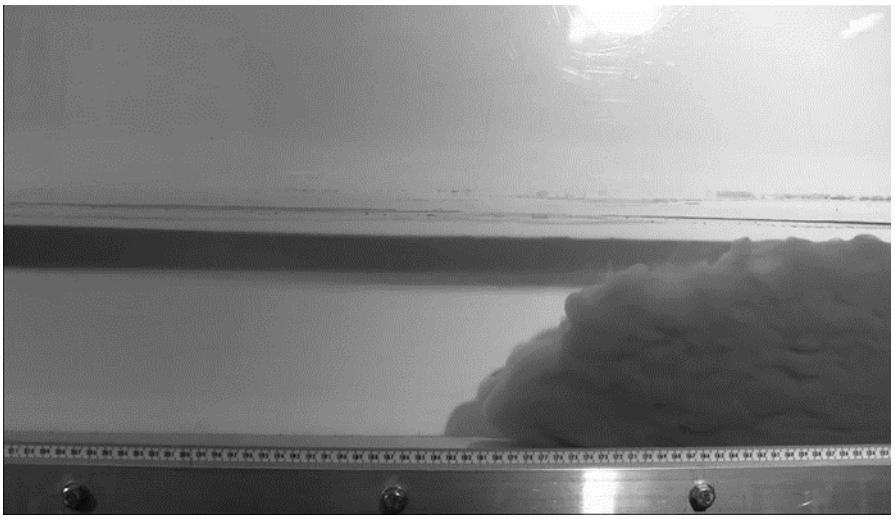

**Figure 17. Image of the suspension of fine material traveling as a turbidity current. The phenomena is likely fine material and relatively low concentration but is effective at moving fine material far out into the flume/pond.**

*Steady State Stage: Growing the BAW*

The steady state stage is the primary condition for operation of tailings storage facilities and, in these experiments, was reached after a few minutes. Once the BAW was established, we observed that the majority of the solids input into the flume were transported over the topset surface. Coarse particles appeared to be transported as bedload along the BAW to the BAW/BBW transition or foreset. Fine particles appeared to be fully suspended in the advected water, i.e. the flowing water over the BAW deposit appeared white in color.

The observations from all four of the surrogate tests suggest that the beginning of the foreset is a critical location within the deposit where the process of transport and deposition dramatically changes. At the foreset position, effectively the end of the beach, the bottom shear stresses developed in the channel flow and which provided conditions sufficient to moved coarse material across the

beach, suddenly decrease. As the channel flow encountered the deeper pond environment, flow velocities drop, resulting in the rapid deposition of solids. For the surrogate mixtures, we observed substantial deposition of the coarse solids on the upper slope of the foreset. As this localized deposit thickened, the foreset steepened and it eventually exceed its natural stability and failed forming a particle avalanche multiple grain diameters thick. The avalanche resulted in a redistribution of particles down the face of the foreset. This process repeated every 10-20 seconds throughout the experiments and appeared to be the primary mechanism for beach growth. We also observed some deposition on top of the beach itself, however, deposition at the forest was the predominant mechanism.

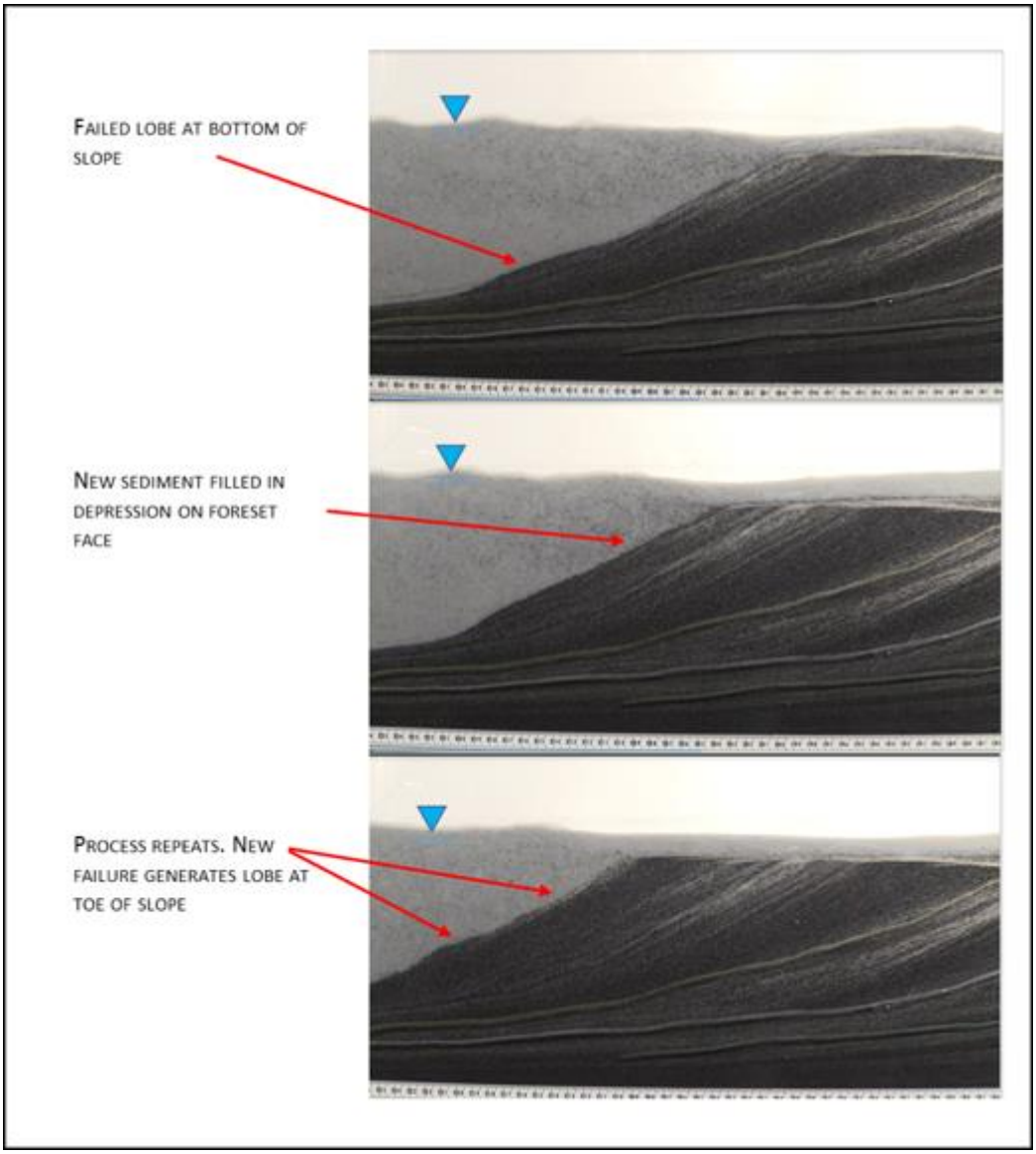


**Figure 18. Time-lapse image from Surrogate Test 5 showing particle avalanche behavior at the foreset. The black material in the image is anthracite and white material is the fine sand. The water surface is indicated on the photographs, which is a suspension of fines including kaolinite. Above the deposit within the flowing fluid, it is possible to see coarse particles carried off the edge of the beach. These particles deposit within the bottomset.**

*Post-Experiment Stage: Settling of suspended solids*

In the third and final stage of the transport, the deposit is formed primarily of the last of the solids to drop out of suspension, the finest particles. In reality, these also get pushed farther and farther into the pond as the beach grows. In the experiments, a portion of this material washed out of the downstream end of the flume.

*Deposit evolution: Surface tracking*

The instantaneous surface of the growing deposit was recorded during an experiment and is referred to here as deposit surface tracking. These data are plotted and shown below for the four surrogate experiments. Figures 19 and 20 are from Surrogate Mixture A and Figure 21 and 22 are for Surrogate Mixture B. Note the vertical exaggeration in the plots. A few observations:

- The initial pond elevation was 15 cm and this elevation controlled the vertical elevation of the end of the beach.
- The slope of the foreset remained consistent throughout the experiments. The build-up and failure of this slopes created some variability but, the average foreset slope did not change during an experiment.
- The BAW slope (topset) also stayed relatively constant however some data indicates the slope decreased with distance from the inlet. This is an effect that is observed on natural deltas and is driven by the fact that, as solids are deposited, the concentration and grainsize of solids of transport sediment load is reduced.
- Surrogate Tests 5 and 6 had complicated bedform features that developed on the beach. We observed upward-migrating bedforms (anti-dunes) resulting in undulating beach surfaces. This can be seen in the deposit surface tracking lines shown in Figures 20 and 21.

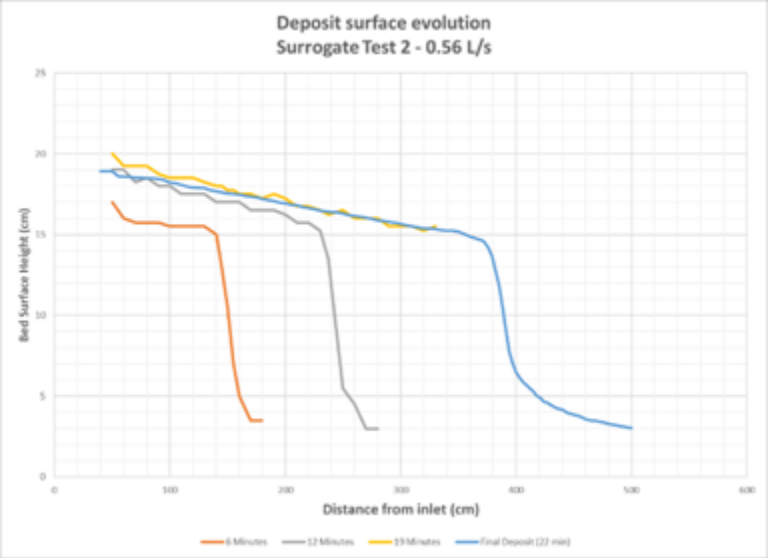


**Figure 19. Deposit surface tracking lines from Surrogate Test 2.**

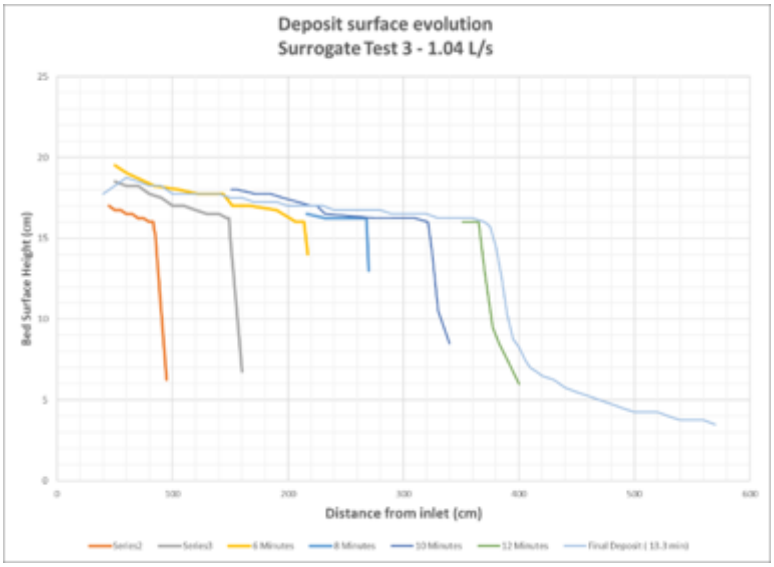


**Figure 20. Deposit surface tracking lines from Surrogate Test 3.**

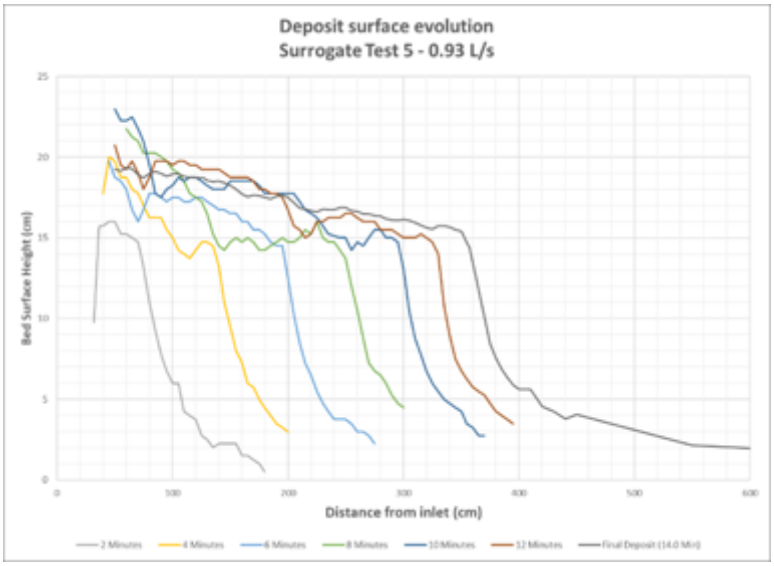


**Figure 21. Deposit surface tracking lines from Surrogate Test 5.**

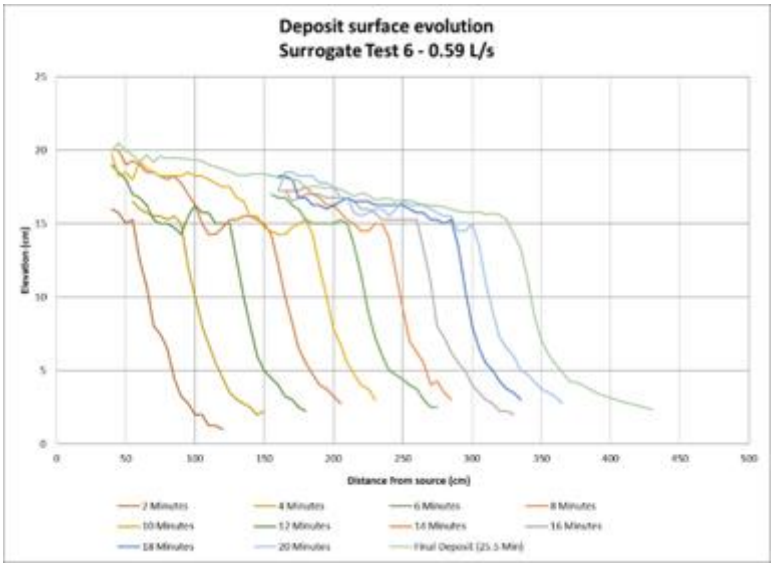


**Figure 22. Deposit surface tracking lines from Surrogate Test 6.**

### *Final surface slopes*

Comparison of the final BAW slopes for the various experiments yield interesting findings. Figures 23 compares beach slope versus discharge for Surrogate Mixture A and suggests that beach slope increases with lower discharge. The same relationship is seen for Surrogate Mixture B, however the relationship is not as strong (Figure 24).

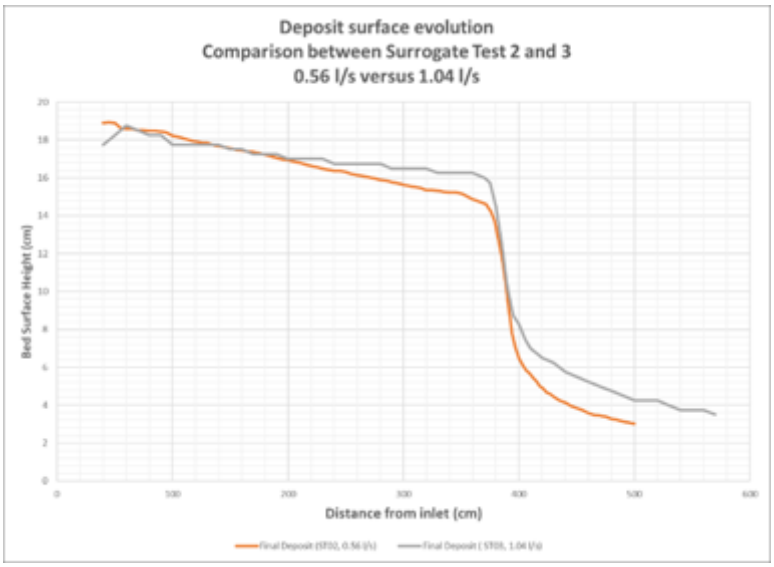


**Figure 23. Comparison of final surface elevation for Mixture A tests (Surrogate Tests 2 and 3).**

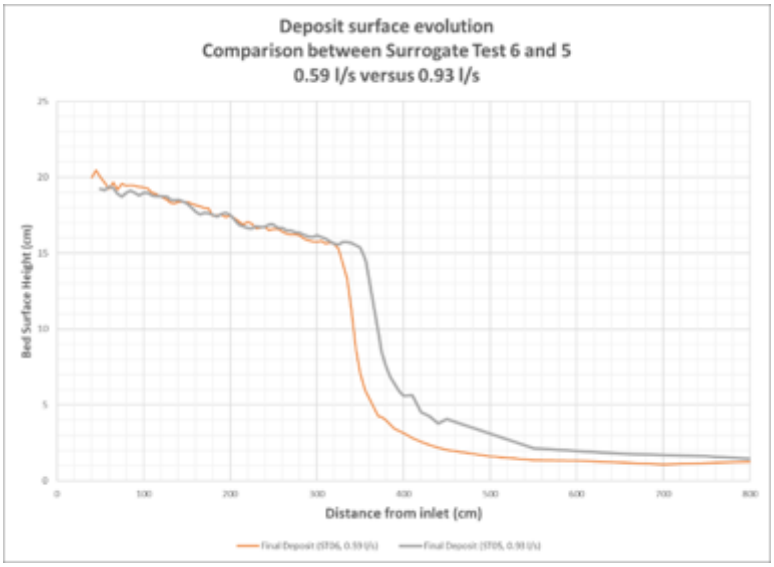


**Figure 24. Comparison of final surface elevation for Mixture B tests (Surrogate Tests 5 and 6).**

Figure 25 provides a summary of the average slopes measured for the four surrogate experiments. Beach (topset) slopes were between 1-2% and decreased with increasing discharge. The foreset slopes ranged from 28% to 40% and also decreased slightly with increasing discharge. Comparing the two surrogate mixtures, Mixture B had higher slopes on both the beach and foreset. The average values for slopes are provided in Table 9.

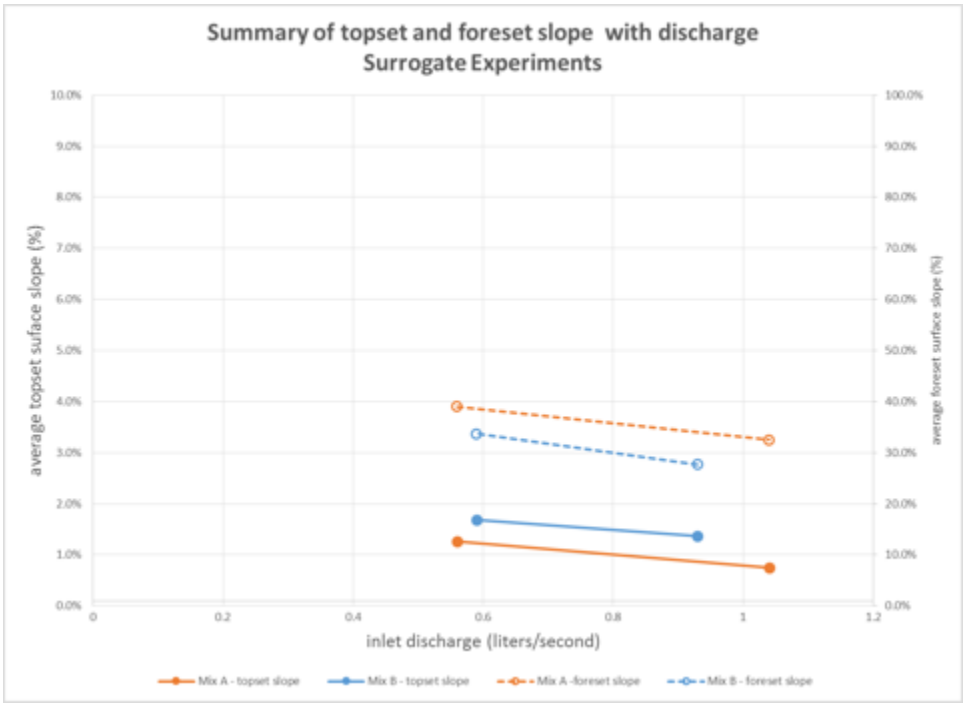


**Figure 25. Summary of the average slopes generated on the beach (topset) and foreset for Mixture A and Mixture B runs. The plots highlight how the slopes change with inflow discharge.**

The foreset and bottom set of the deposit represent the Beach Below Water (BBW) and are shown comparatively in Figure 26. In this figure, the x-axis is the relative position of the deposit using the start of the foreset as zero. The elevation data is also adjusted by a scalar using the elevation of the top of the foreset in Surrogate Test 2 as the basis. In other words, the measured elevations of foresets for Surrogate Tests 3-5 were shifted up or down by a scalar such that the elevation of the forests all begin at the same relative elevation. The four tests are plotted together for comparison and reveal several characteristics:

- The slopes of the foresets are all very similar for these tests as is verified in Table 9.
- The higher discharge runs have higher relative elevation at the toe of the foreset and a thicker bottom set deposit.

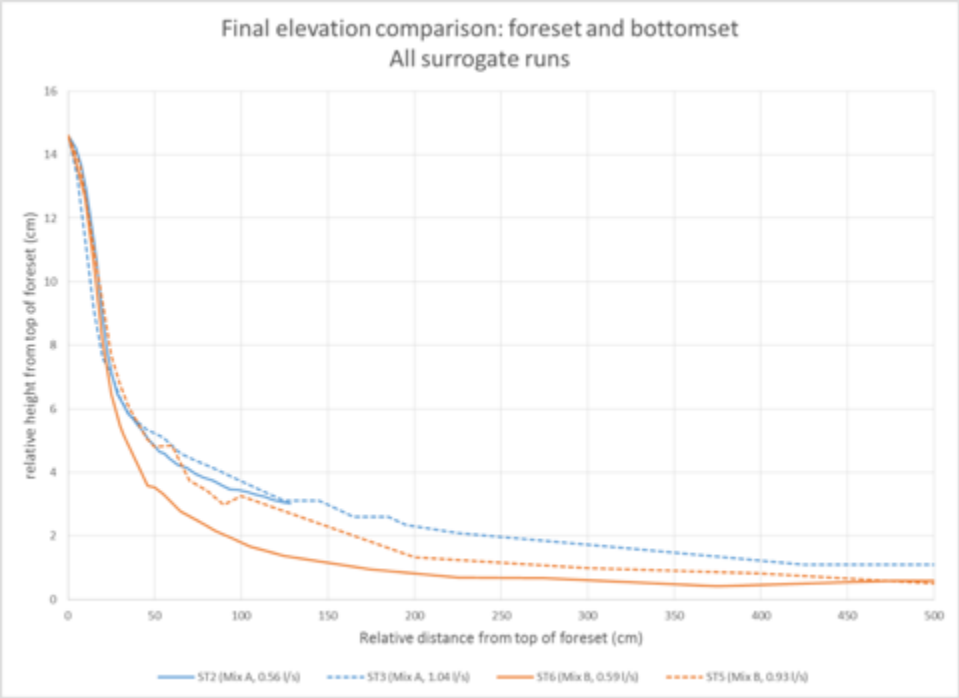


**Figure 26. Comparison plot of relative elevation for BBW deposit for all four surrogate tests.**

### *Flow depth, velocity and bed shear stress*

The video recordings of the surrogate experiments were used to estimate flow depth over the beach for the four experiments and these values are reported in Table 9. Average beach and foreset slope are also included in this table. Using this information, it is possible to calculate an estimated bed shear stress using the relationship defined in equation (1).

$$\tau_b = \rho g H S \qquad (1)$$

Where,

$\tau_b$ = bed shear stress
$\rho$ = fluid density
g = gravitational acceleration

H = average flow depth
S = average beach slope

The resulting bed shear stresses suggest that Surrogate Tests 2 and 3, which used Surrogate Mixture A, adjusted to a bed shear stress ranging between 1.4 -1.7 $N/m^2$. Similarly, Surrogate Tests 5 and 6 (Mixture B) self-adjust to a bed shear stress of 2.4 $N/m^2$.

**Table 9. Summary of slope and velocity data. The table also includes an estimate of the average bed shear stress generated by the flow over the beach.**

| Experiment | Beach Slope (-) | Foreset Slope (-) | Discharge (l/s) | bulk density (kg/m3) | gravity (m/s2) | depth (m) | bed shear stress (N/m2) |
|---|---|---|---|---|---|---|---|
| Surrogate Test 2 | 0.0126 | 0.390 | 0.56 | 1032 | 9.81 | 0.013 | 1.66 |
| Surrogate Test 3 | 0.0075 | 0.325 | 1.04 | 1032 | 9.81 | 0.019 | 1.44 |
| Surrogate Test 5 | 0.0137 | 0.277 | 0.93 | 1061 | 9.81 | 0.017 | 2.42 |
| Surrogate Test 6 | 0.0168 | 0.337 | 0.59 | 1061 | 9.81 | 0.014 | 2.45 |

### *Deposit images and video*

Digital video cameras were used to capture transport and deposition processes associated with the four surrogate tests. Edited videos are available through the project website and submitted to the project sponsor as a deliverable (https://sites.google.com/umn.edu/uminncosia-tsru-tailings-resea/home?authuser=2). A few key images are provided below.

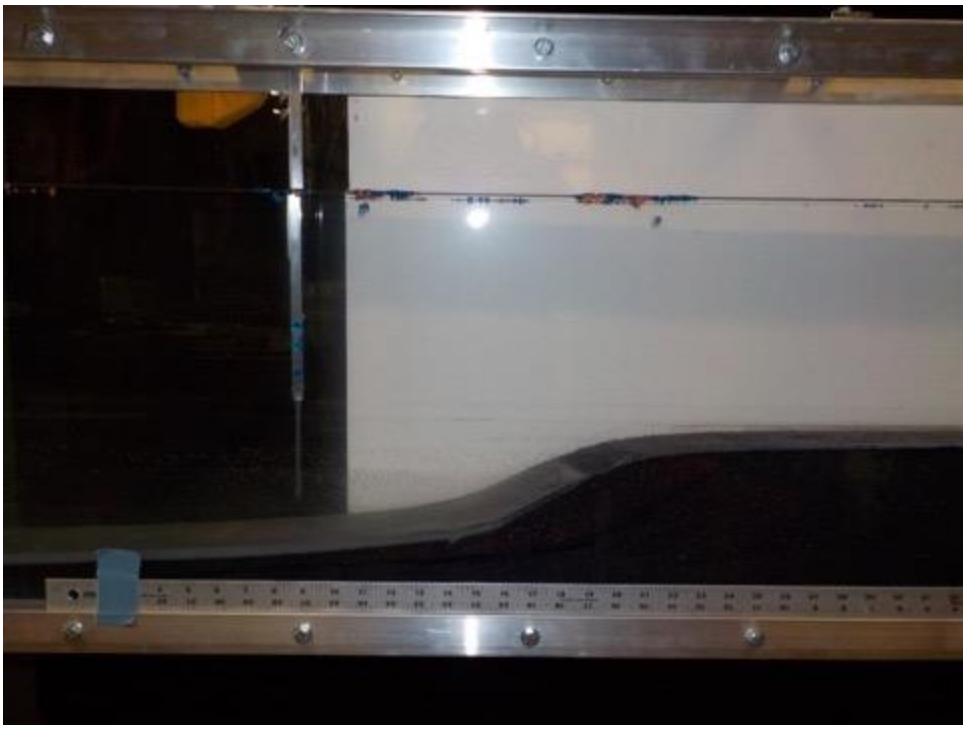

**Figure 27. Image of the final deposit of the Surrogate Test 2 showing the foreset. The deposit is submerged under tap water as the final deposit survey is underway.**

**Figure 28. Image taken of the final deposit several hours after the end of Surrogate Test 3. The water surface is at the end of the beach. A fine grained solids layer (grey) can be seen draping the bottom set deposit resulting from suspension settling.**

*Grainsize variability in the final deposit*

All four surrogate tests involved post-test sampling using a lab-scale piston coring method. This method was described earlier in this report. Cores were extracted and subdivided into three layers, top, middle and bottom. The three layers were intended to correspond with the three mechanisms responsible for deposition: the top layer corresponding to beach surface process; the middle layer corresponding to foreset growth (particle avalanching); and the bottom layer corresponding to deposition by particle settling.

In general, nine coring location were determined including three on the beach, thee at the foreset and three downstream of the foreset. Each core was sub-divided into top, middle, and bottom yielding 27 sediment samples per test. Samples were analyzed on a Horiba Laser Analyzer 920.

The results of the coring are presented in terms of a grainsize histogram with grainsize on the x-axis and frequency of occurrence on the y-axis. Studying the vertical and streamwise variation in the grainsize distribution reveals relationships between the mixture composition, transport mechanisms and deposition.

Figures 29 to Figure 32 summarize all the grainsize data collected from the cores and are presented along with deposit surface tracking plots for the runs. Figure 29 is data collected in Surrogate Tests 2. As a reminder, the top row of grainsize plots describes the grainsize variation of the top of deposit. For these BAW, the transport processes were largely fluvial (e.g. suspended load, bed sheet load, bedload transport). Foreset and bottom set grainsize at the top shows an increase in finer material.

The middle grainsize plots are associated with the foreset growth (particle avalanching). Within the BAW, the particles sizes are fairly constant however foreset and bottom set data suggest an increase of fines trapped within the deposit.

The bottom grainsize plots are associated with the settling processes of the fine-grained material and start forming far from the moving foreset. Fine material that washed off the beach settles out of the

pond and onto this layer. As the experiment progresses, the foreset and topset advance over the bottom set effectively trapping this layer. The grainsize data confirms the bottom layer is finer grained than the upper two layers. Figure 30, 31, and 32 are similar presentations of grainsize variability over the experimental deposit.

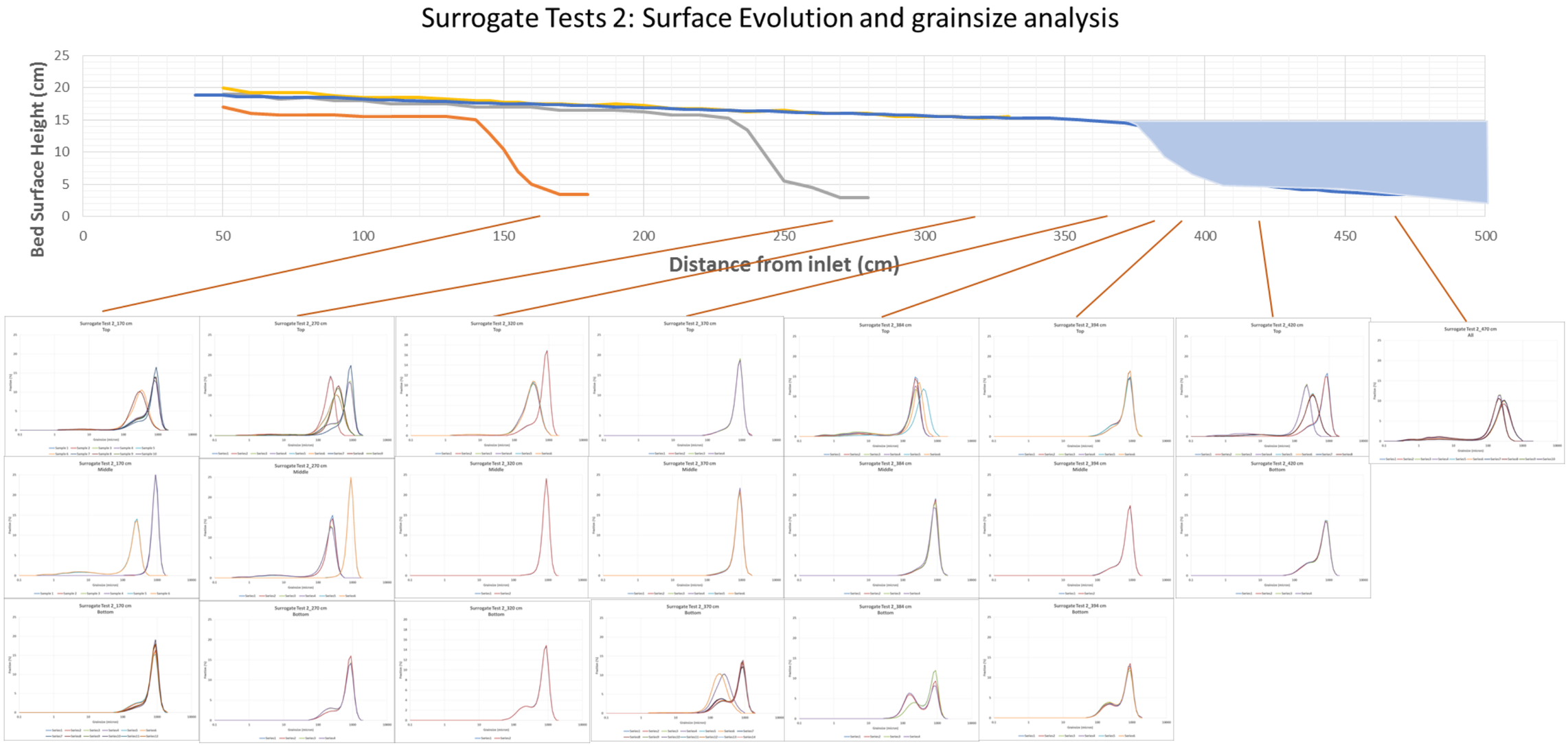


**Figure 29. Comprehensive summary of grainsize distribution of the deposit formed in Surrogate Test 2.**

# Surrogate Tests 3: Surface Evolution and grainsize analysis

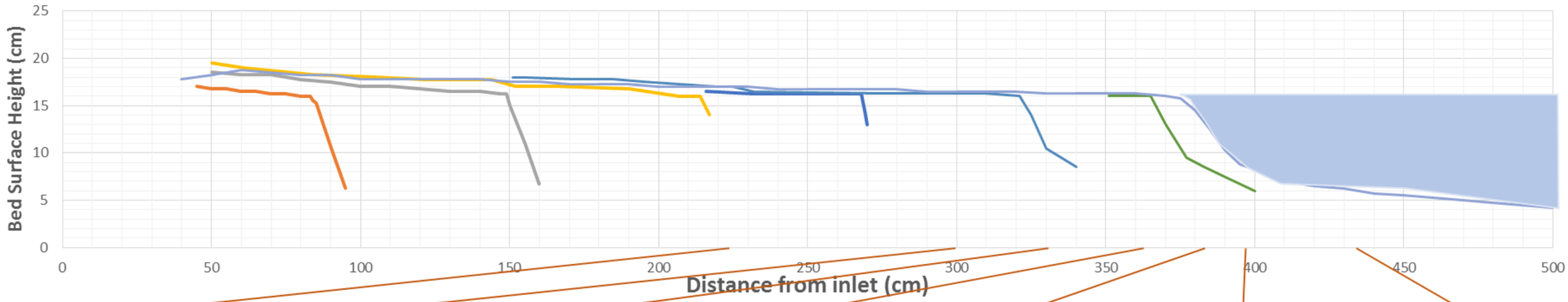


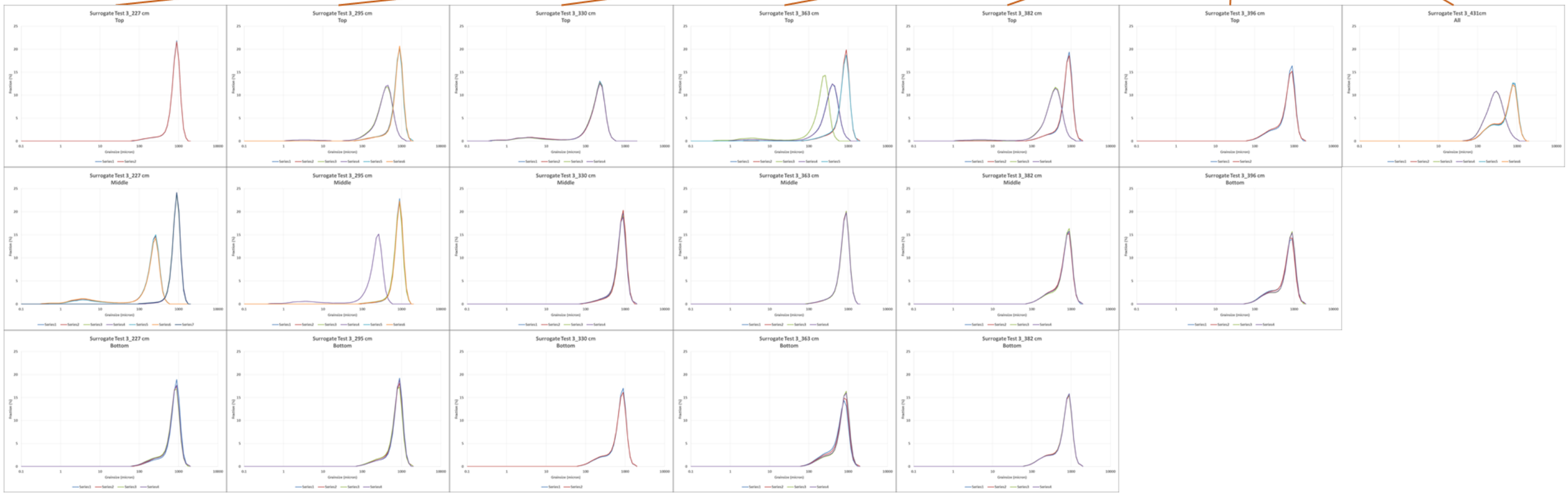

**Figure 30. Comprehensive summary of grainsize distribution of the deposit formed in Surrogate Test 3.**

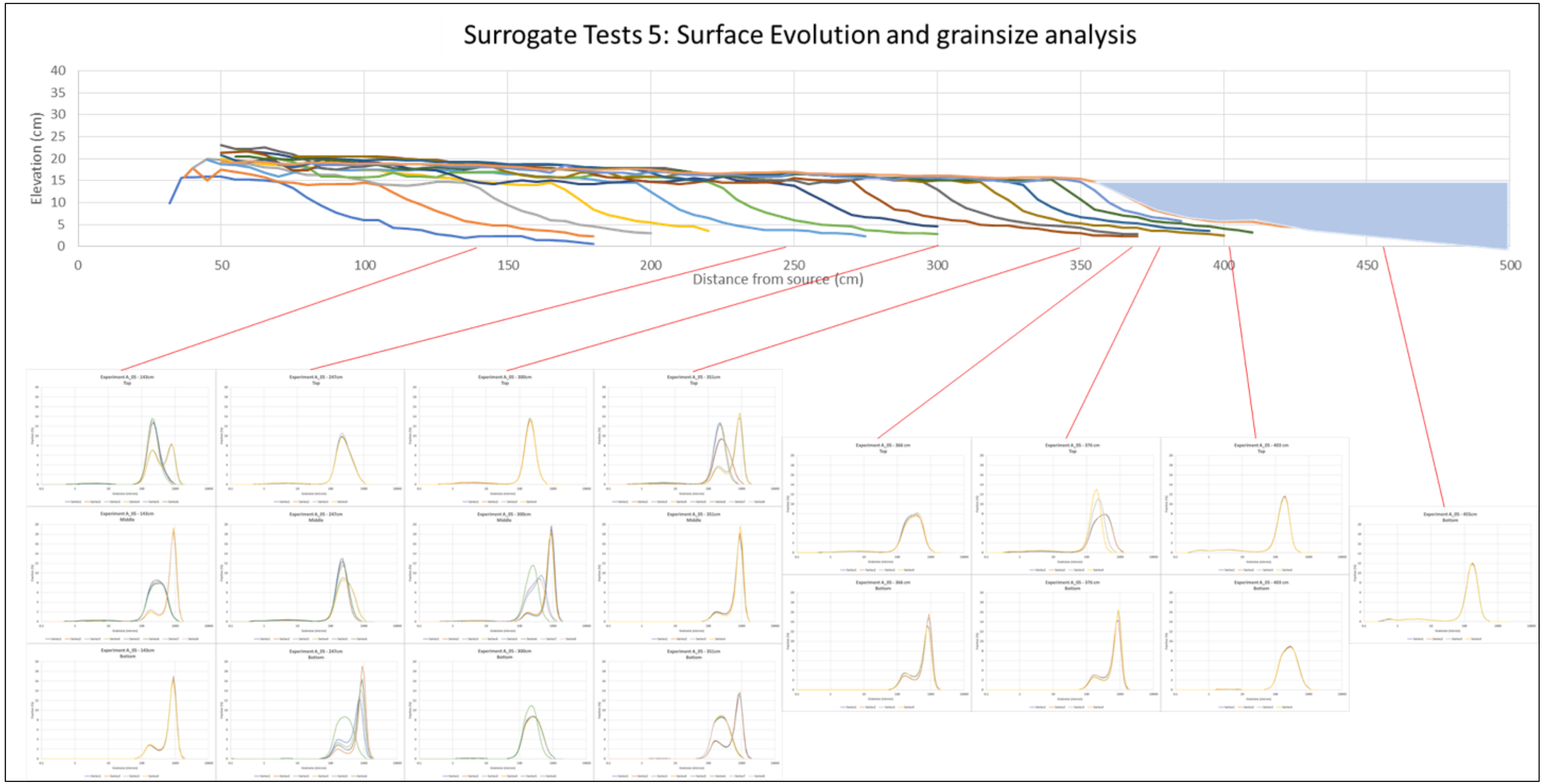


**Figure 31. Comprehensive summary of grainsize distribution of the deposit formed in Surrogate Test 5.**

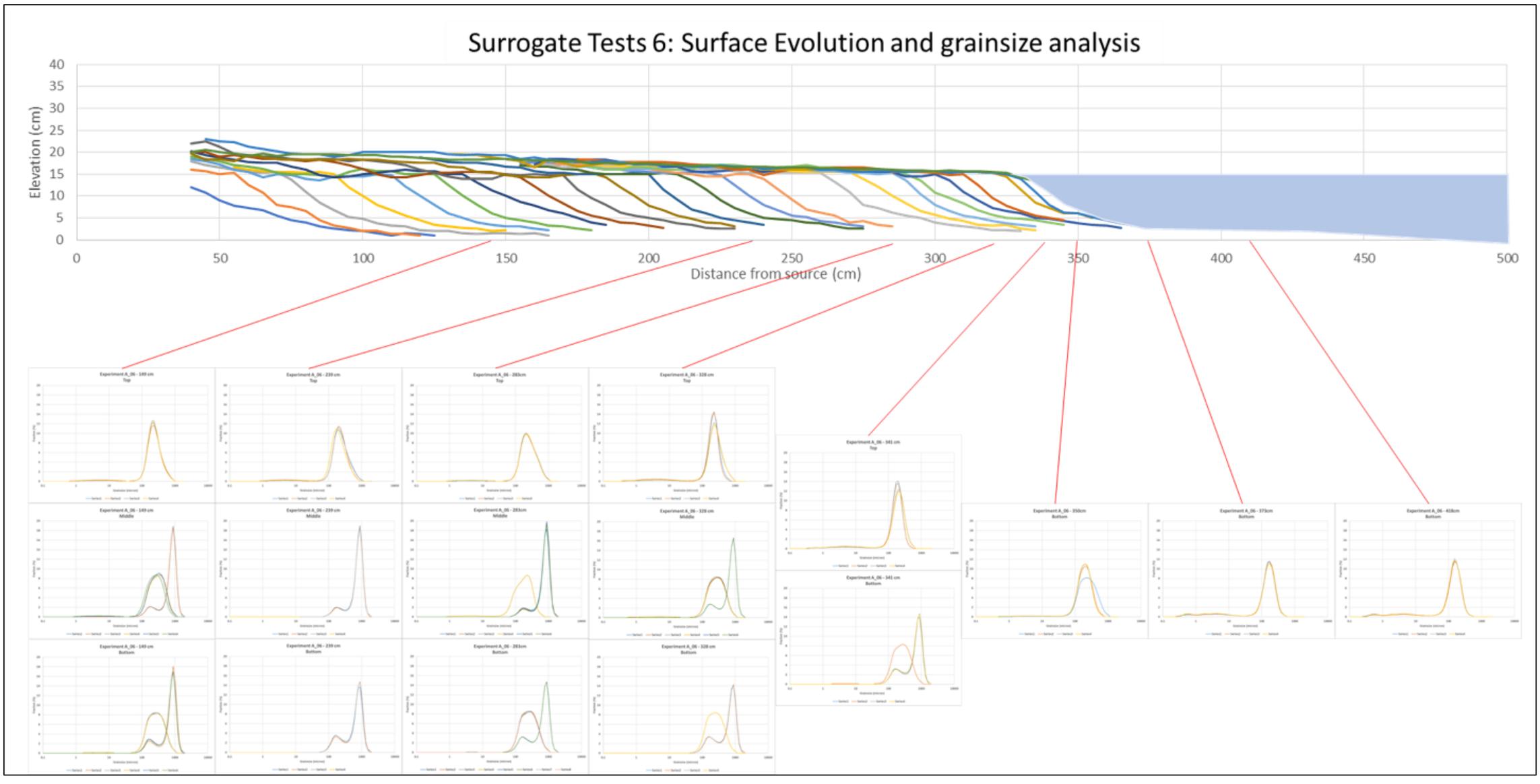


**Figure 32. Comprehensive summary of grainsize distribution of the deposit formed in Surrogate Test 6.**

# PHASE 2 - TSRU TAILINGS EXPERIMENTS

## Overview

Phase II involved experiments using real TSRU tailings. High Temperature (HT) TSRU tailings material was provided by COSIA member, Imperial Oil. Three distinct experiments were conducted at varying input discharge rates and utilized the same facility as described above with slight modifications to the mixing and delivery systems. The data acquisition/data collection systems were also identical. Table 10 summarizes the three experiments and attributes.

## Test Material

The tailings were provided by Imperial Oil in Alberta Canada and delivered to UMN in October of 2018. The shipment included six 1 $m^3$ totes of TSRU tailings, and three 1 $m^3$ totes of process water. It is not known when the samples were collected at the field site or the manner in which they were collected. The tailings samples were likely collected at elevated temperature and cooled to room temperature while in the totes. TSRU tailings and process water were disposed of according to waste disposal protocols of the University of Minnesota.

We note here that the experiments were performed at 20 °C. Extensive conversations with the Project Stewards explored the issues around elevated temperature of the TSRU tailings and effect of this temperature and cooling within the tailings pond on the final deposit and pond characteristics. Because this project is the first effort working with the TSRU tailings in a moderate scale laboratory experiment, our focus remained on the behaviors of room temperature TSRU tailings.

### *Material Mixing and Delivery*

The TSRU tailings segregates relatively quickly and needed to be mixed prior to introducing into the experimental flume. Several iterations of mixing design were attempted before a final design was implemented. Figure 33 shows an image of the setup used for mixing and delivery for the TSRU tailings experiments. A large, cylindrical tank was procured and installed near the research flume. Internal baffles were installed along the perimeter of the tank, extending the full height of the tank and providing conditions for optimal mixing. A variable speed motor-mixer was installed into the tank and served to provide mixing energy to the tank. The open top of the tank was covered with pink panel insulation to prevent evaporation and contain odor. This insulation was removed as needed to collect suspended sediment samples from the mix tank (Figure 34).


**Figure 33. Images of the mixing tank used for TSRU tailings experiments. A large variable speed mixer with long shaft was added. Internal baffles were installed on the perimeter of the tank as well.**

**Figure 34. Image of mixing vessel prior to a TSRU experiment. Pink insulation was used to cover the tank and was slid to the side in order to collect samples from the tank.**

A centrifugal pump was used to drive additional mixing in the tank and deliver material to the research flume (Figure 35). The inlet to the pump withdrew material from the bottom of tank and pumped it up ~3 meters above the floor and returned it to the mixing tank, creating a closed-loop pumping circuit. Prior to the experiment, the pump was allowed to continually withdraw and re-circulate this material back into the mixing tank, which aided in the keeping the tailings fully suspended in the mixing tank and preventing settling in the delivery pipe network. A plumbing "T" and PVC pipe were connected to this recirculation line and routed to the constant-head supply tank over the research flume. A series of valves allowed the research team to adjust flow rate delivered to the flume as described earlier in this report.

**Figure 35. Image of the centrifugal pump used to deliver TSRU tailings to the research flume.**

As discussed previously, a manually operated constant-head tank was installed over the research flume. This portion of the setup was identical to Phase I. Because the elevation of the tailings slurry in the supply tank changes over the duration of the experiment, the hydraulic performance of the pump changed thus requiring continual adjustment of the inlet valve to achieve a constant influent flow rate. Figure 36 is an image of this setup including the constant head tank into the flume.

**Figure 36. Image of mixing tank (background), recirculation plumbing and constant head tank leading tailings slurry into research flume.**

## Summary of Data Collection and Sampling

The data collection program was nearly identical to Phase 1 and included the following elements.

- Discharge measurement
- HD video cameras
- Deposit surface tracking
- Suspended sediment sampling
- Still photographs
- Final surface elevation surveys
- Deposit coring and analysis

## Results

This section summarizes the data and results from the Phase 2 research.

### *Flow discharge, flow durations, and volume/mass added.*

Table 10 summarizes the average influent discharge and the duration of each experiment. The lowest flow rate, experiment T_02, was 0.25 l/s with a duration of 18.6 minutes and 524Liters of tailings slurry (water and solids) introduced into the experiment. T_01 was an intermediate influent discharge of 0.47 l/s with a duration of 20.7 minutes and total volume of tailings slurry of 524 liters. The highest influent flow rate was T_03 with 0.96 l/s and a duration of 11.4 minutes. Total volume of tailings slurry introduced was 656 liters.

The flow rates were determined using the sharp-crested weir at the end of the flume. Experiment duration was measured during the run and verify by analyzing the audio recorded on video cameras. Total volume was calculated as the product of experiment duration and influent flow rate.

**Table 10. Summary of Phase II experiments. Influent discharge was the primary independent variable in these experiments.**

| Experiment | Discharge (Liters/second) | Total Volume (Liters) | Duration (Minutes) | Equivalent unit discharge (l/s-m) | TSRU tailings bulk density ($kg/m^3$) | Total estimated mass solids added (kg) |
|---|---|---|---|---|---|---|
| T_01 | 0.47 | 524 | 18.6 | 4.7 | 1075 | 81 |
| T_02 | 0.25 | 311 | 20.7 | 2.5 | 1075 | 46 |
| T_03 | 0.96 | 656 | 11.4 | 9.6 | 1075 | 114 |

### *Observation of transport processes*

Digital video recordings of the experiments were reviewed and evaluated. The video provides important insights into linkages between transport, solids segregation, and deposition. Here we provide a summary of observations broken down over three regions of the deposition formation, the Beach Above Water (BAW) deposit (topset), the transition zone between BAW and Beach below water (BBW) (foreset), and the BBW deposit (bottomset).

*BAW processes*

The extents of this region extend from the flume inlet to the shoreline, which is continually advancing away from the inlet. Figure 37 is a four-panel image summary taken from the videos. The following observations are highlighted:

- The initial condition for each experiment was a quiescent 15-cm deep pond of process water, clear of particles. Upon introducing tailings material into the flume, a gravity current/turbidity current formed along the bottom of the flume (A). As the turbidity current moved through the flume, sediment was observed falling out of suspension and depositing on the bed. This was most pronounced near the entrance of the flume.
- The deposit thickened quickly near the upstream end of the flume and eventually reached the pond elevation and emerged as a subaerial fluvial flow. A shallow slope formed and the beach deposit began to form and grow. As the beach grew in length, a depositional front formed that represented the end of the BAW deposit (B). Off-shore, that is, beyond the shoreline, we observed turbulent flow and continuation of the turbidity current to the end of the flume.
- We observed the consistent formation of a thick froth deposit in the first 200 cm of the flume. The froth was heavily air-entrained and seemed to float on the flowing TSRU tailings. The froth seemed to have enough mass that it became a pseudo upper boundary for the flowing tailings.
- As the beach advanced farther down the flume, the elevation of the beach continued to increase indicating that a portion of solids entering the flume were depositing on the beach surface. This was less true under the thick froth layer where most of the solids were bypassed downstream (C).
- Later in the runs, complex interactions were observed between the flowing tailings, the solids deposit on the beach and the overburden of froth. Bedform features began to emerge and translated downstream; the beach deposit had an undulating appearance (D).

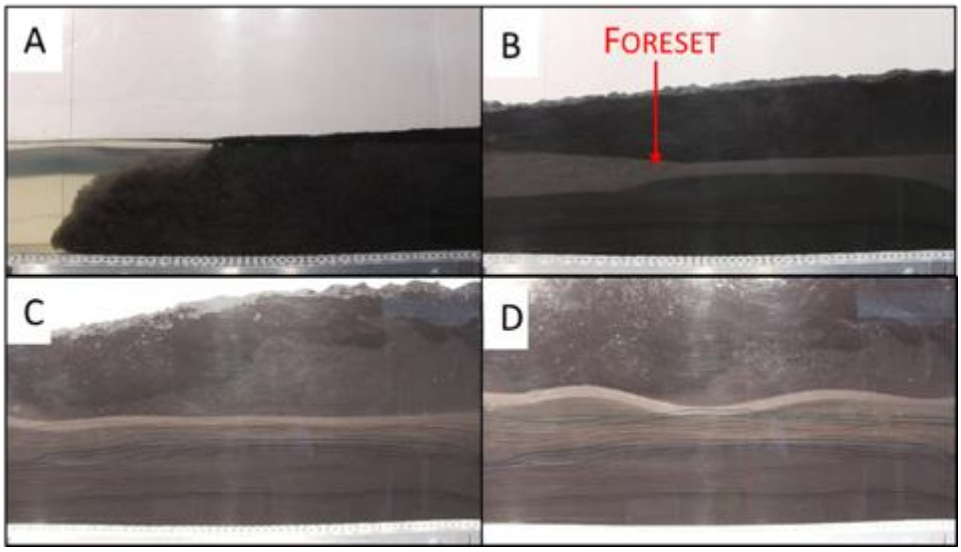


**Figure 37. Four-panel summary from video data taken in experiment T_01 near the entrance of the flume. Flow is from right to left. The images A-D show the evolution of the beach deposit.**

*BBW Processes*

Observations farther out in the pond suggest the bottom turbidity current played an important role forming the BBW deposit. Figure 38 is a four-panel image summary of processes observed offshore of the beach. Again, flow is from right to left.

- Images A through D represent the flow and deposition with varying distances from the shoreline where A is farthest from the beach and D is the closest. Beach position is indicated with red arrows.
- In all images, a sediment laded turbidity current was present along the bottom of the pond. This suspension of solids was continually fed by water and solids leaving the BAW zone. The material was denser than pond water and thus sank to the bottom of the pond and flowed to the end of the flume. Turbulence in the flow served to keep fine and/or light particles in suspension and transported them far from the shoreline into the pond.
- The slope of the BBW deposit increased with proximity to the shoreline, i.e. the bottom slope in panel A is shallower than in panel D.
- Vertical velocity profiles are included in the panels and are drawn qualitatively from the video images. In A, far from the shoreline, the bottom turbidity current existed on roughly the bottom half of the pond depth and the upper half was relatively quiescent. In B and C, as the deposit thickened, the zone of quiescent pond shrank until the turbidity current reached the free surface.

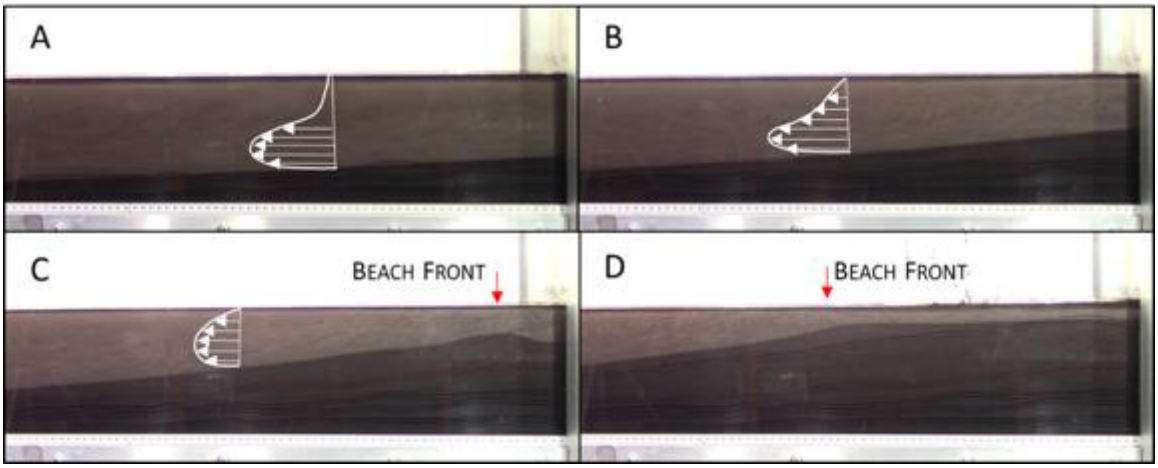


**Figure 38. Four-panel summary from video data taken in experiment T_02 at mid-flume (300 cm). Flow was from right to left. The images A-D show the evolution of the BBW deposit. The beach front position is indicated with a red arrows. Estimated vertical velocity profiles are drawn in panels A-C to illustrate the turbidity current active on the bottom of the pond. As the elevation of the deposit thickened, the turbidity current began to interact with the free surface of the pond.**

*BAW/BBW transition – the shoreline*

The transition zone (or foreset) was dominated by similar processes as observed in the surrogate runs. Solids that reached the end of the BAW zone deposited at the top of the shoreline. Over time, the local deposit steepened and catastrophically failed. Grains slid or avalanched down the face of the slope – spreading out along the face, resulting in the progradation of the beach. Kinematic sorting was observed here where segregation of coarser material toward the deposit-fluid interface

occurred, and the finer segregated away from the deposit/fluid interface. The finer particles thus deposited sooner, closer to the water surface, and the coarsest material segregated to the bottom of the slope. This process was continuous over the duration of the experiment. Figure 39 is a two-panel summary of the foreset from experiment T03.

- While the processes of deposition and avalanching is similar to that observed in the surrogate runs, the vertical height of the forest is smaller with TSRU tailings. The foreset height in A and B is on the order of 5-8 cm in height compared to Surrogate Tests in which the foreset height was nearly the full pond depth of 15 cm.
- It appears that deposition of solids from off-shore processes associated with the turbidity current have a larger role in the TSRU tailings experiments. That is to say, for surrogate tests, the beach was primarily formed by deposition at the foreset and on the topset whereas in TSRU tailings, we observe a thicker deposit formed in the pond from settling out of a turbidity current.

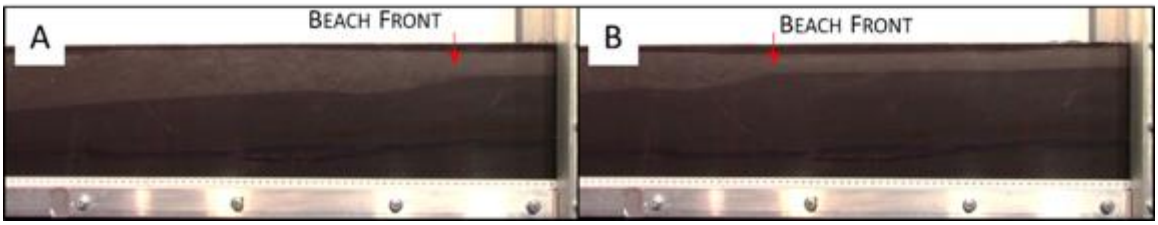


**Figure 39. Two-panel image summary from experiment T_03 of the prograding shoreline. Image A and B are separated by roughly 60 seconds.**

*Flow velocity with distance from source*

The research team evaluated video data to determine average depth of the flow over the BAW region of the deposit. By assuming continuity of flow over the length of the beach, we calculated average flow velocity with distance from source (Figure 40). Except for a region from 0-200 cm, where froth formed over the deposit and created a region of pseudo-conduit flow, the average velocities appeared relatively constant. Velocity also increased with influent flow rate.

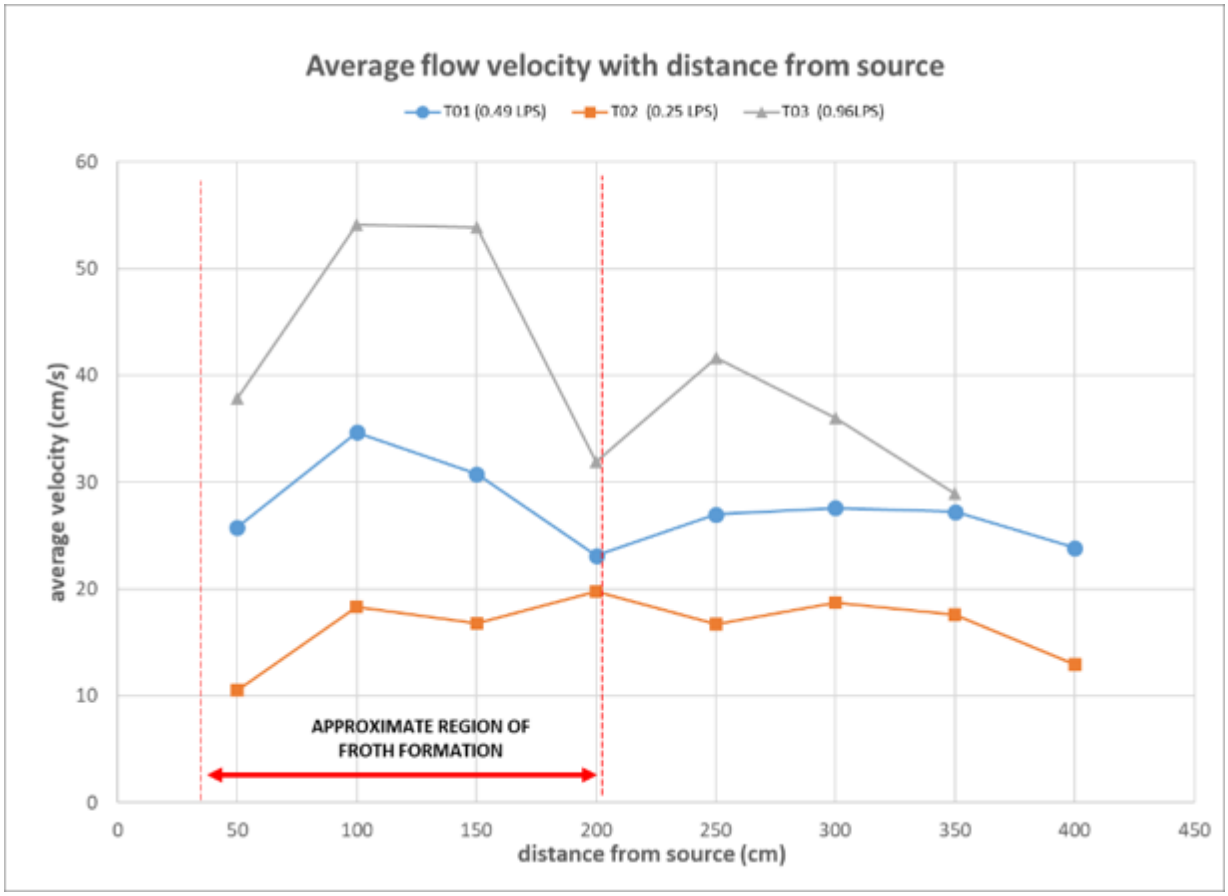


**Figure 40. Summary of average flow velocity with distance from the source for the TSRU tailings experiments.**

*Final Deposit Images*

Digital photographs were taken of the final deposit and the images were stitched together to create a final composite photo of the deposit. The images are presented in this section.


**Figure 41. Composite images taken of the final deposit of T_02 (input discharge = 0.25 l/s). Flow was from right to left.**

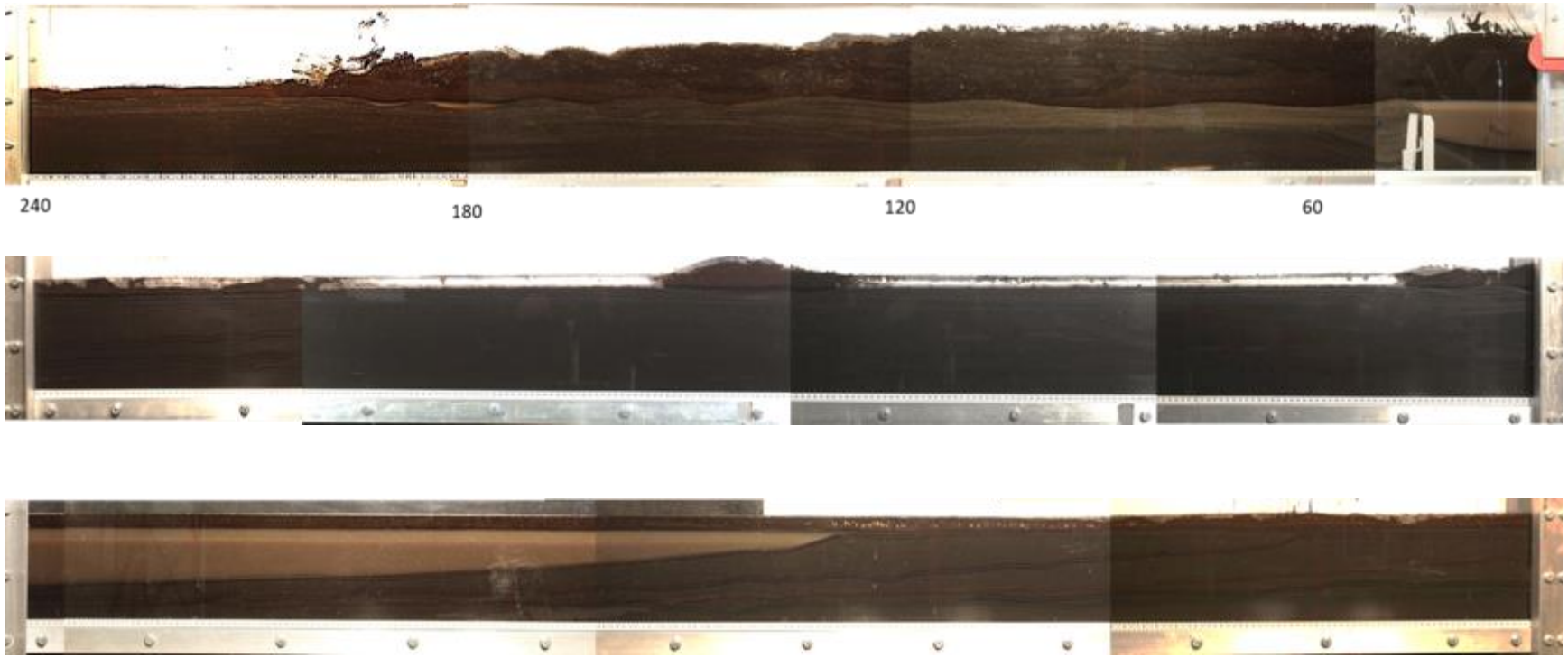


**Figure 42. Composite images taken of the final deposit of T_01 (input discharge = 0.46 l/s). Flow was from right to left.**

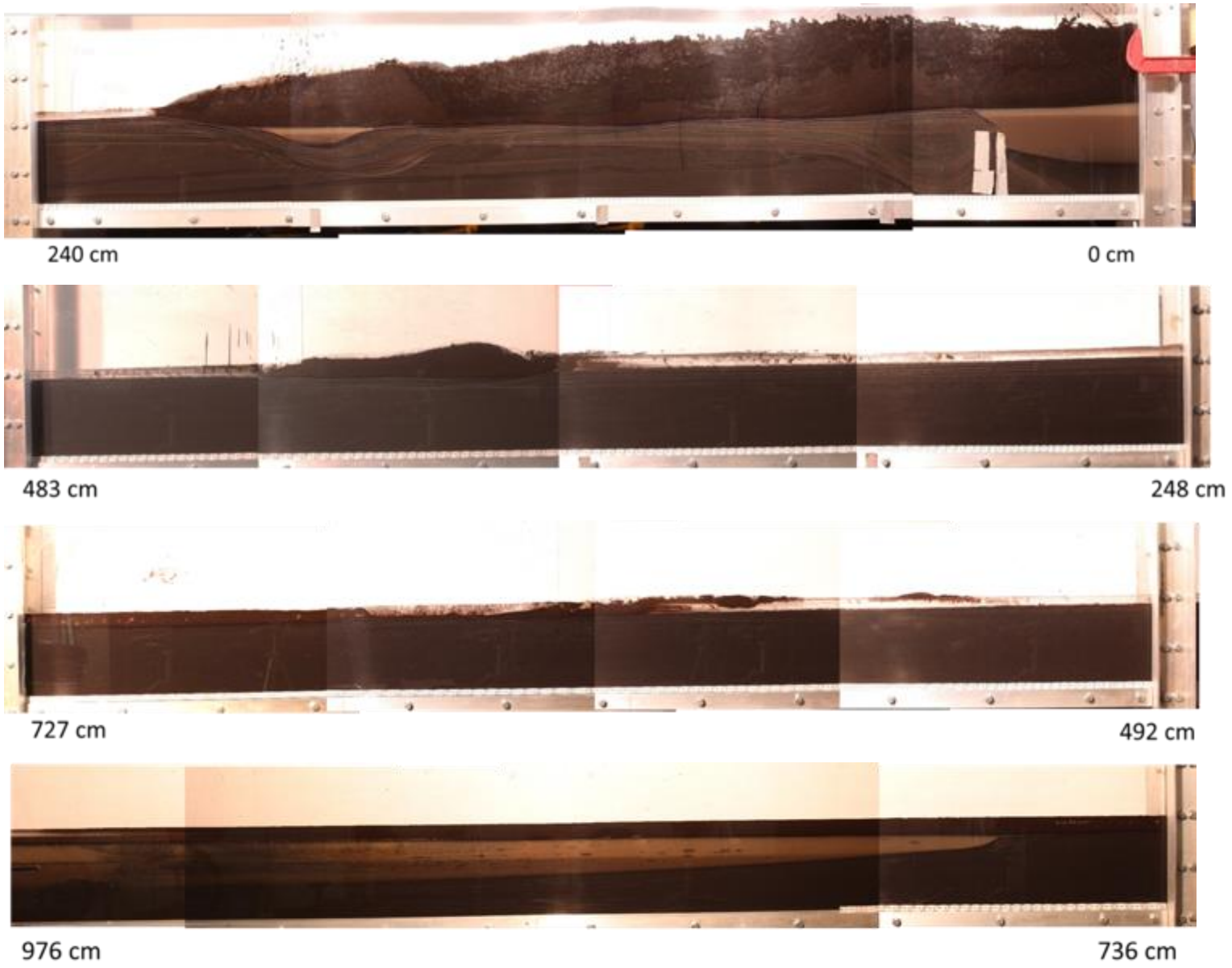


**Figure 43. Composite images taken of the final deposit of T_03 (input discharge = 0.97 l/s). Flow was from right to left.**

*Evolution of the deposit and final deposit geometry*

In all three TSRU tailings experiments, the initial pond elevation was filled with process water and set to a fixed elevation of 15-cm depth. At periodic intervals, the research team recorded the instantaneous deposit elevation on the glass window of the flume and these lines were later measured and recorded. Figure 44 compares the topographic evolution of the deposit over the duration of each of the three experiments, where flow was from left to right. A few important observations can be made:

- The inflow rate was the primary independent variable for Phase 2. The plots in Figure 44 are ordered from lowest discharge to highest. The lowest discharge also had the smallest mass of solids added to the flume. The length of the beach is not linked to the inflow rate but resulted from the total mass of materials fed into the flume. Interestingly, experiment T_03 resulted in the longest beach but was the shortest duration experiment; this clearly shows the total mass added to the flume is a critical parameter in beach size.
- Surface tracking lines also included the final surface of froth. Figure 48 clearly shows the size and extent of froth over the three experiments. For the 0.47 l/s and 0.96 l/s experiments the surface tracking lines under the froth stack on top of one another indicating no deposition occurred during these time intervals and the solids bypassed this region with no net deposit. Surface elevation lines appear to even have a positive slope under the froth. This supports observation made in the video.
- The higher discharge experiments generated froth islands. These were observed to be discrete chunks of the main froth island that broke away and floated downstream where they became lodged mid-flume. Scour was also observed under the froth islands.

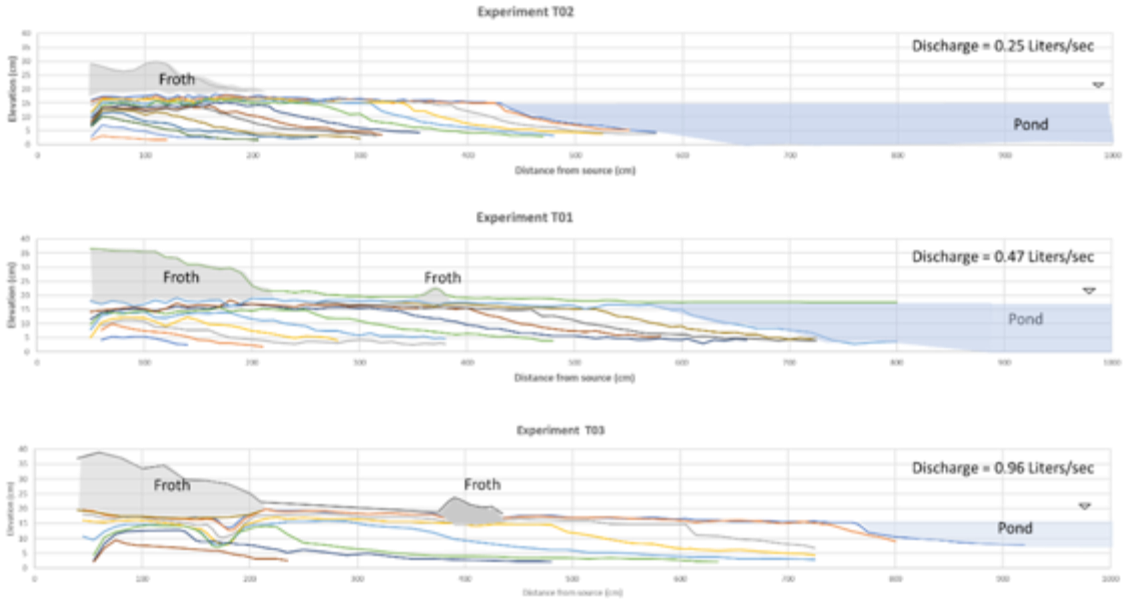


**Figure 44. Three plots showing the evolution of the deposit surface over the course of the experiments.**

Analysis of the final surface survey data allowed estimation of final slopes of BAW, BBW and the foreset. Average slopes for these three regions are plotted in Figure 45. The BAW slope calculation

only considered the region beyond the froth islands. These slope data are interesting in that they represent a self-formed characteristic. As in rivers, the equilibrium or average slope of the channel represents the gradient necessary to balance the ability of hydraulics to move solids and the tendency for solids to settle on the bed.

The BAW slopes decreased slightly with increasing discharge and ranged between 0.9% and 0.7%, which was also observed in the surrogate tests. Through communication with project stewards, the BAW slopes of TSRU tailings beaches in the field environment are between 1.5-3% (Correspondence, K. Rudolf, CNRL). A second source of information suggested BAW slopes are 0.5% (Correspondence, M. Graham, CNRL). It appears, however, that very little data on BAW TSRU tailings slopes is available. The fact that the laboratory measured slopes are within this range is a validation that the full-scale unit discharge was an appropriate parameter for designing the experiments.

BBW slopes also decreased with increasing discharge. This is perhaps due to the formation of a more energetic turbidity current that is able to transport solids farther into the pond. Project stewards report that field BBW slopes are around 10% (Correspondence, M. Graham, CNRL), which is again in the range of what was measured in the laboratory experiments. BBW slopes for surrogate s were not recorded.

Foreset slope increased with increasing discharge from 29% to 40%, which is opposite of the surrogate tests.

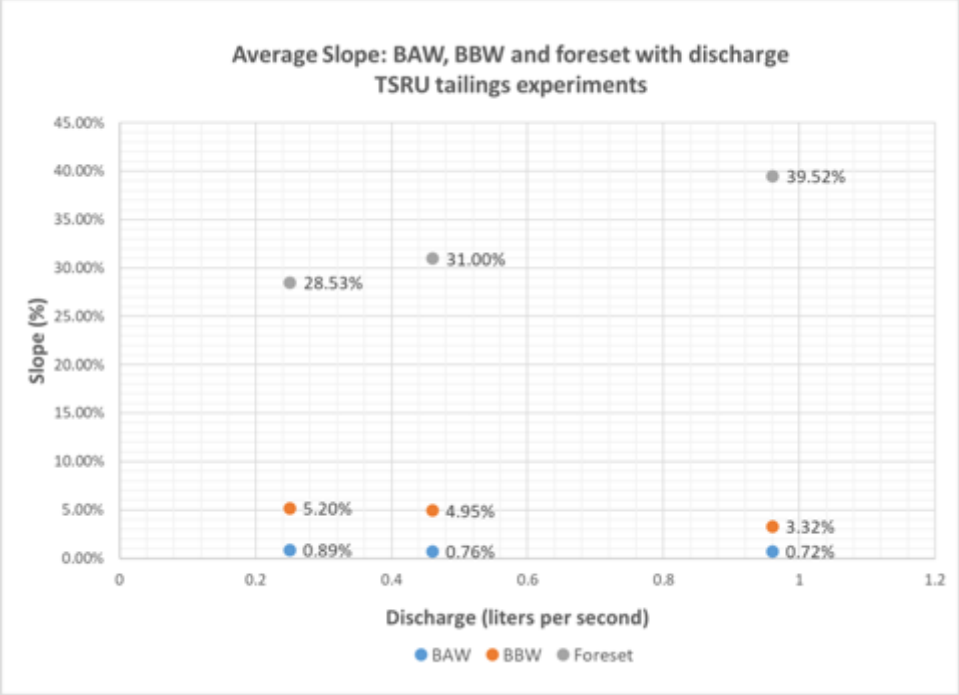


**Figure 45. Summary of average slopes computed from final surfaces of the three TSRU tailings experiments. Discharge for the three runs were: T_01 (0.47 l/s), T_02 (0.25 l/s), and T_03 (0.96 l/s).**

### *Solids segregation and final deposit characteristics*

After the completion of the experiment, the research flume was allowed to sit for several hours while surface survey data and still photographs were collected. Survey data was used to determine the nine locations for sediment coring, which were then extracted from the deposit. The cores were kept in a vertical orientation and frozen until analysis. Each core was subsampled into three layers

corresponding to the zone of deposition that produced the deposit. The top layer was generated by the topset, the middle layer by the foreset, and the bottom layer by bottomset. Samples were then analyzed on a Horiba L920 Laser Diffraction machine.

Samples were analyzed in the same state they were extracted from the flume. That is, the samples did not go through any pre-treatment to remove bitumen or coal material (e.g. Dean Stark method was not employed) and so the results represent the particle size distributions (PSD) of solids as they were transported in the flume.

Figure 46 is an example of the three-panel PSD plots generated for the cores and are a useful way to visualize the variations observed in grainsize. The sample location is provided in the figure header. The data show a bimodal distribution of material with peaks around 10-30 micron and 100-200 micron. A larger proportion of sand sized material (>44 micron) was found in the middle and bottom layers. The data also suggest that, comparing the bottom and middle layer there was a decrease in the 10-30 micron material in the bottom layer.

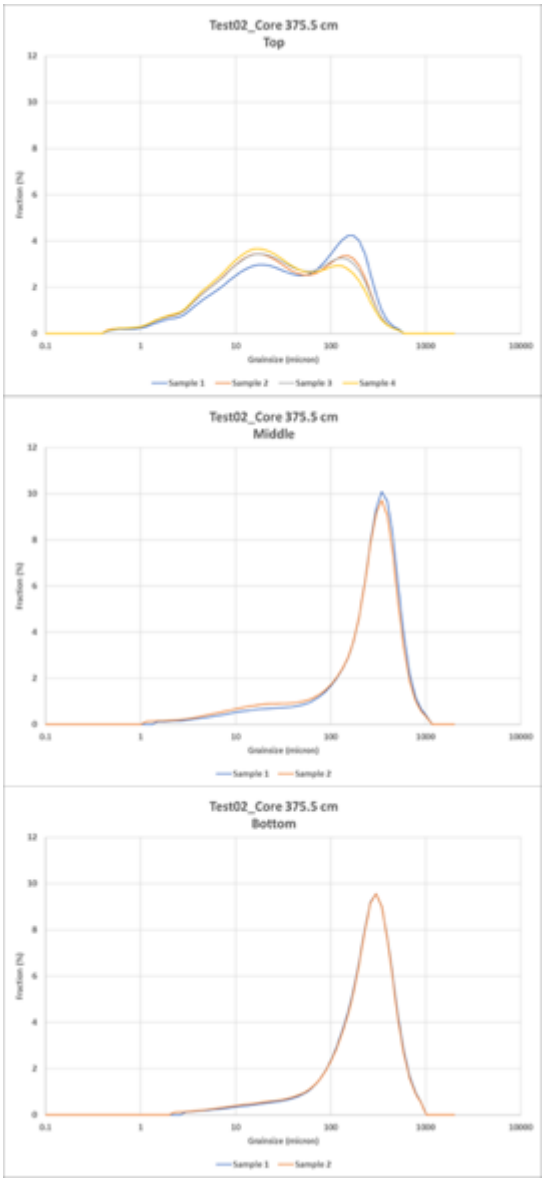


**Figure 46. Three panel summary of the PSD analysis of a core. Each core was subsampled into a top, middle, and bottom layer. Subsample PSDs were processed several time and plotted as a histogram. The plots are oriented as extracted from the core (i.e. top, middle, and bottom).**

Three-panel PSD data was developed for all cores collected and assembled in stream-wise order (Figure 47 -Figure 49). Core location is tied to the final deposit geometry in the figure to help with interpretation. The figures are order by increasing influent discharge (i.e. Figure 47 is the lowest discharge and Figure 49 is the highest discharge).

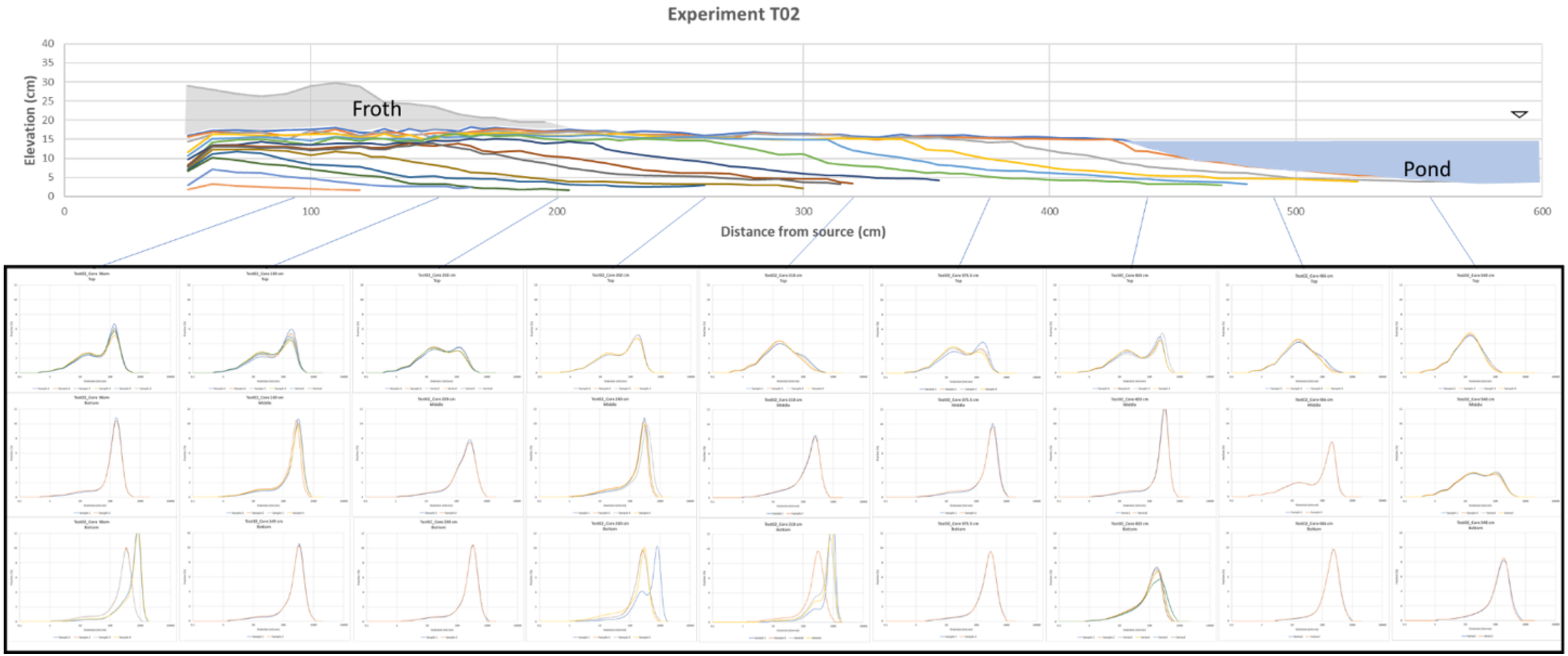


**Figure 47. Sediment core PSD data collected for T_02 (inlet discharge = 0.25 l/s). Core position is referenced to the final deposit geometry.**

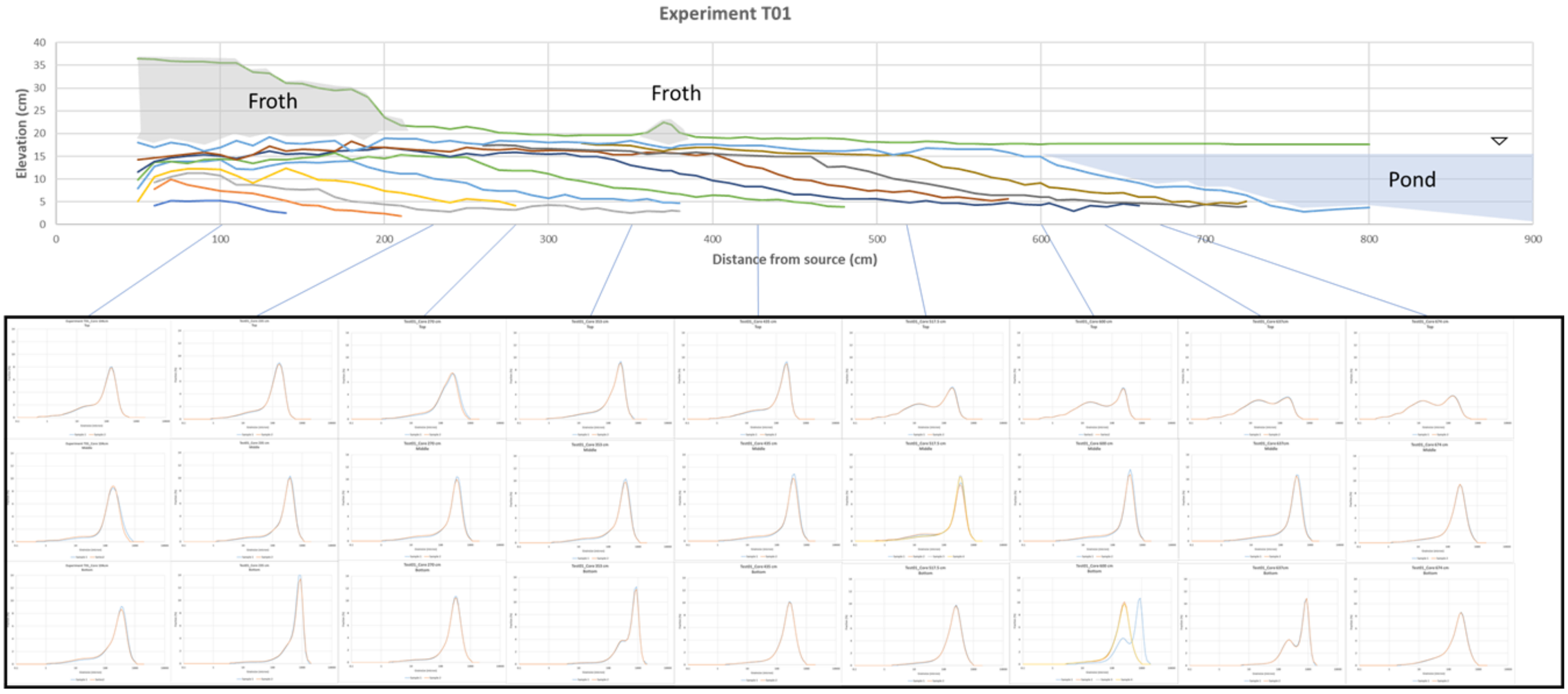


**Figure 48. Sediment core PSD data collected for T_01 (inlet discharge = 0.47 l/s). Core position is referenced to the final deposit geometry.**

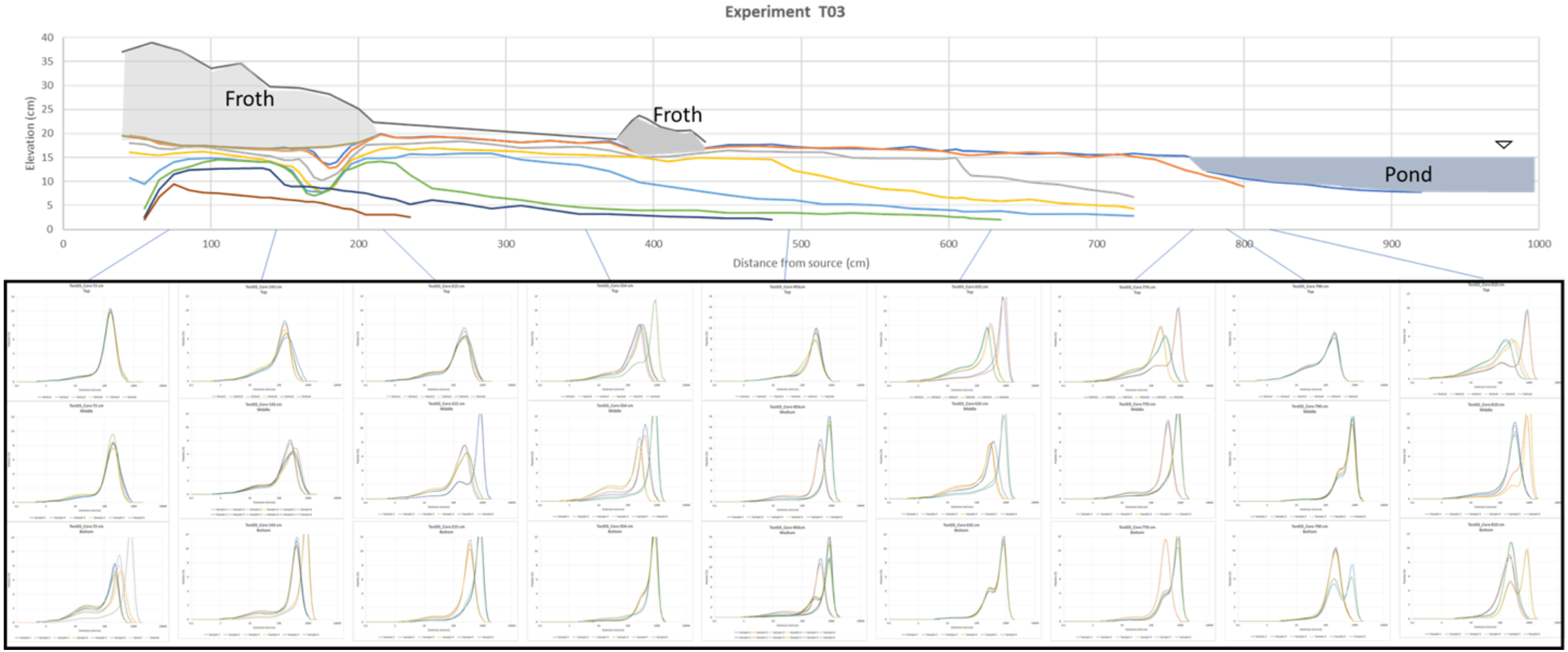


**Figure 49. Sediment core PSD data collected for T_03 (inlet discharge = 0.96 l/s). Core position is referenced to the final deposit geometry.**

PSD data were further analyzed by determining the equivalent mass fraction of solids that were within the sand size range or greater (>44 micron). Figure 50 summarizes these data from the three TSRU tailings test, ordered from lowest discharge to highest. Recall that a froth layer formed from 0-200 cm in all three tests and this is marked on the figures. The shoreline position at the end of the experiment is also shown in the figure. The y-axis represents the %wt of solids greater than 44 micron, considered the sand content.

The following observations are made from the data shown in Figure 54:

- The initial sand content of tailings sampled at the inlet to the flume was 58% by weight and is indicated as the yellow point on 0.47 l/s plot. The sand content is defined as the percentage of solids mass with a particle size greater than 44 microns.
- The grainsize variation of the bottom cores are attributed to solids that settle out of the pond water far from the beach front. For two of the experiments the particles size in these cores decreased with distance from the inlet. In other words, these cores had a decreasing sand content with distance from the inlet. Less sand was able to make it farther into the pond. This was true for the 0.25 l/s and 0.47 l/s experiment but was not detected for the 0.96 l/s experiment, which showed a steady sand content in the bottom cores around 80%. We also note that the magnitude of sand content increased with discharge in the bottom sample. For the 0.25 l/s test, sand content in the bottom layer had a maximum value of around 60% however reached 80% for the 0.96 l/s test. In summary, higher discharge resulted in higher sand content with the BBW and the sand was carried farther out into the pond.
- We note that the sand content for all data are higher than the initial sand content at the inlet. This is likely attributed to the fact that the proportion of fines is actually reduced resulting in a higher sand content. The fines are removed by the energetic flow.

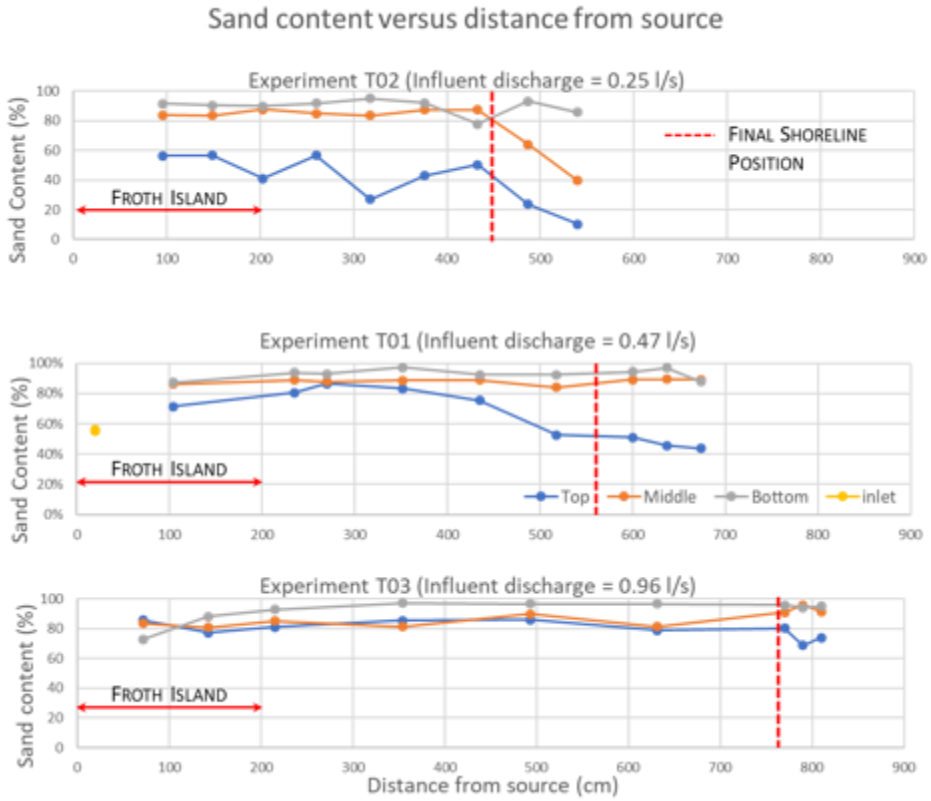


**Figure 50. Summary of sand content measured in the sediment cores for the three TSRU tailings experiments.**

*Suspended sediment sample and segregation of tailings stream*

Small grab samples (~125ml each) were taken at regular intervals during each of the TSRU tailings experiments to determine the properties of the suspended sediment at these locations. Sampling locations included the mixing tank, inlet to the flume and surface samples collected approximately 15-cm off the shoreline of the BAW. Froth sample were also collected. These samples were processed for solids content and bulk density and a small set of samples were analyzed for PSD using the laser diffraction machine.

Table 11 summarizes inlet solids content and shoreline suspended sediment concentration. The average inlet concentration was relatively consistent between the three runs ranging from 14-16 %wt. solids, where solids content is measured as: (mineral solids + bitumen)/(total weight). Solids content measurement at the shoreline position was very steady at 9%. It is interesting that suspended sediment concentration at the end of the beach did not vary with discharge.

Using this data, we can compute estimates for the proportion of material solids fed into the flume that remain in the beach or flowed off the beach. Data suggest that there is an inverse relationship between solids captured in the beach and discharge.

**Table 11. Summary of suspended sediment analysis for the three TSRU tailings experiments.**

| Experiment | Influent Discharge (lps) | Average inlet concentration (%wt) | Suspended sediment concentration at shoreline (%wt) | Fraction of total solids flowing off the beach (-) | Fraction of solids captured in topset (-) |
|---|---|---|---|---|---|
| T02 | 0.25 | 13.6% | 8.8% | 64.9% | 35.1% |
| T01 | 0.47 | 14.3% | 9.0% | 62.6% | 37.4% |
| T03 | 0.96 | 16.2% | 9.2% | 56.8% | 43.2% |

Table 11 does not partition solids between sand and fines. A small number of samples were collected in the test and analyzed for grainsize. This differs from the core deposit PSD data shown earlier as these are data for solids suspended in the inflow, off the end of the beach, or within a froth layer. Figure 51 shows a summary of particle size data from the T_01 experiment. The data were repeatable and consisted and reveal interesting trends when plotted together. The solids suspended in the froth layer are fine grained with a peak ranging between 10-40 micron. The inlet samples reveal a bimodal distribution with peaks at 10-30 micron and 100-200 micron. Shoreline suspended samples mirror inlet samples however have a higher proportion of fine material to sand sized material.

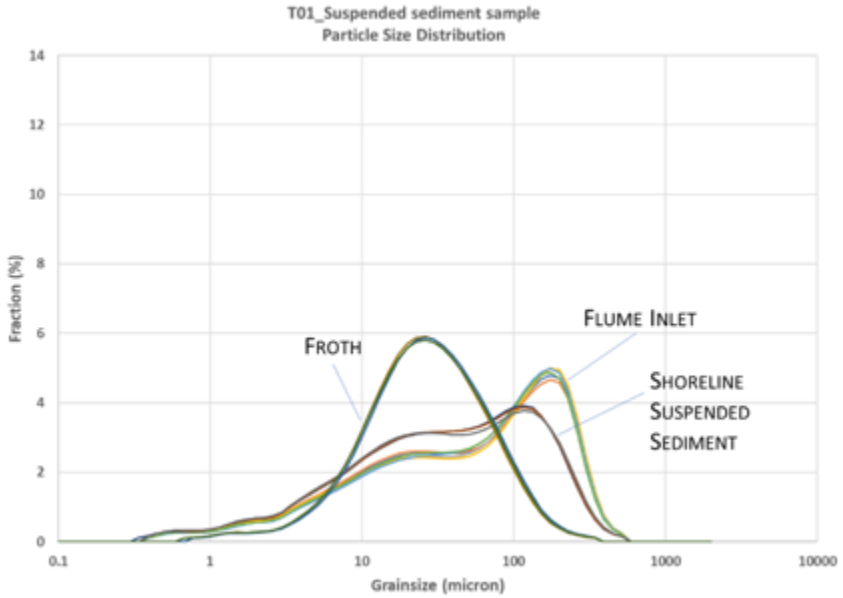


**Figure 51. Summary figure showing PSD data generated from laser diffraction analysis of sediment samples. This data is from the T_01 experiment (0.47 l/s) and samples from surface froth and suspended sediment samples captured at the inlet to the flume and from the shoreline grab samples of flow leaving the beach.**

## *Evaluation of TSRU Segregation*

**Using data collected from surface suspended sediment and deposit bathymetry, it is possible to evaluate the proportion of solids, by mass, the entered the flume and where they ended up in the deposit.**

Table 12 is a summary of this analysis.

The total mass added to the flume was determined by multiplying the measured influent flow rate, influent bulk density and experiment duration. Bulk density was measured in the lab using standard procedures resulting in an average of 1075 g/liter.

The estimate of mass of material deposited in the beach zone used several data sets. Here, we seek to estimate the mass of material contained in the region upstream of the final shoreline. Final deposit survey data and flume width were used to determine the volume occupied in the beach. Because the deposit is formed by discrete particles as well as complex silts, clays and asphalting particles that contain water, we apply a porosity to the deposit. Here we select 0.6 based on the fact that the deposit was surveyed moments after the end of the run with little time for dewatering and compaction. To convert from a volume of solids to mass of solids, a deposit density of 1500 g/liter was applied. This value was measured from core samples collected in the beach area of experiment T_03 using standard procedures. The total mass fraction contained in the beach was computed as the ratio of the mass in the beach over the total mass of solids added during the experiment.

**The data suggest that the percent of total mass captured in the beach deposit decreased with increasing discharge. An important clarification is needed here based on the discussion of video of the transport and depositional processes. We observed visually that a substantial bottomset was formed in the TSRU tailings experiments. Over time, the foreset and topset would build out over the bottomset deposit. Therefore, what is measured here in the "beach deposit" is an assemblage of the three zones of transport that collectively form the beach deposit. The results from**

Table 12 suggest that as we increased discharge, a greater mass of material was able to avoid capture within the beach; more material moved farther out into and out of the flume. At lower discharge, material may have moved off the beach and into the pond but a high fraction of this material became incorporated into the beach.

The final analysis in Table 12 is an estimate of the mass of solid that was carried off the end of the beach. The source data for this analysis are the surface grab samples collected ~15cm downstream of the shoreline. The average bulk density of these samples was ~1040 g/liter. Assuming the volumetric flow rate remained constant over the beach and multiplying by the bulk density and duration of the experiment, the total mass exported off the end of the beach (water and solid) was determined. The solids content of the surface grab samples was also measured and had an average value of 9%wt. The solids content multiplied by the total mass yielded the total mass of solids exiting the beach.

The data suggest that, as discharge increased, the fraction of solids leaving the beach area decreased. If we assume that material not washed off the beach areas was captured on the beach surface or topset, the results suggest that at higher discharge, more material was captured in the topset deposit than at lower discharges. This result may seem counterintuitive until we consider the role of the froth in the experiment. In general, a strong layer of froth formed for all three of these tests. Solids content

of the froth was not measured however we know that the froth contained fine grained solids. It follows that the froth served to segregate fines from on the topset and this is reflected in the lower percentage of total solids leaving the beach. The segregation by the froth increased with increasing discharge.

**Table 12. Table summarizing estimated mass balance from the three TSRU tailings experiments.**

| Experiment Name | T_02 | T_01 | T_03 |
|---|---|---|---|
| ***Total mass of solids added to experiment*** | | | |
| **Flow Rate (liters/second)** | **0.25** | **0.47** | **0.96** |
| Experiment duration (seconds) | 1244 | 1116 | 683 |
| Experiment duration (minutes) | 20.7 | 18.6 | 11.4 |
| Total volume (liters) | 311 | 525 | 656 |
| TSRU Bulk Density (g/liter) | 1075 | 1075 | 1075 |
| Total mass of water and solids added (kg) | 334.3 | 563.9 | 704.9 |
| Average solids content at inlet (% wt) | 13.6% | 14.3% | 16.2% |
| **total mass of solids added (kg)** | **45.5** | **80.6** | **114.1** |
| ***Estimated mass fraction in beach zone*** | | | |
| Length of beach (cm) | 430 | 600 | 765 |
| Deposit volume assuming no pore space (liters) | 63.2 | 95.4 | 123.4 |
| Assumed deposit porosity | 0.6 | 0.6 | 0.6 |
| Volume of solids (liters) | 25.3 | 38.2 | 49.4 |
| Solids particle density (g/liter) | 1500 | 1500 | 1500 |
| Total mass in beach (kg) | 37.9 | 57.2 | 74.1 |
| **Percent of total solid mass (%)** | **83%** | **71%** | **65%** |
| ***Estimated mass off the end of the beach*** | | | |
| Bulk density of flow at end of beach (g/liter) | 1040 | 1040 | 1050 |
| Total mass flux (g/s) | 260 | 488.8 | 1008 |
| experiment duration (second) | 1244 | 1116 | 683 |
| Total mass off the end of beach (g) | 323.4 | 545.5 | 688.5 |
| Average solids content off beach (% wt) | 0.088 | 0.09 | 0.09 |
| Total solids mass off end of beach (kg) | 29 | 48.8 | 63.2 |
| **Portion of solids mass off end of beach (%)** | **63%** | **61%** | **55%** |

### *Froth formation*

The volume of froth generated in each was measured. This can be seen in the surface plots shown in Figure 44. The froth volume occupied in the flume for each run was 11.2 liters, 20.6 liters and 21.9 liters for runs T_02, T_01, and T_03, respectively. It was difficult to estimate the mass of solids contained in the froth since the air content or void volume was not measured. Our observation was

however that the froth contained the fines fraction of the solids (Figure 51) and was an effective mechanism for segregating fines out of the tailings slurry.

**Figure 52. Various images of the surface froth formed in the TSRU tailings experiments.**

## Conclusions

In this report we provided a detailed summary of two phases of experiments investigating the transport, segregation, and deposition of TSRU tailings materials. In Phase 1, we explored this space using two surrogate mixtures (A and B) that differed by the addition of a fine sand that effectively widened the PSD of the surrogate. Two discharges were evaluated for each of the mixtures (~0.5 and 1.0 l/s). In Phase 2 we performed experiments using real TSRU tailings. The primary independent variable in these experiments was the influent flow rate (0.25, 0.47 and 0.96 l/s). Multiple types of data were collected during these experiments that, when analyzed together, provide unique insights into the transports and segregation process and how these result in the BAW and BBW deposits.

#### TSRU tailings deposition has three regions of distinct transport, segregation, and deposition

The BAW, BBW and BAW/BBW Transition were discussed in detail in terms of their transport, segregation, and deposition physics. Suspension and moderately-dense shear layers with dynamics sieving were primary mechanisms forcing a segregation of solids by size and density. The BAW/BBW Transition was a region of dramatic change in both hydraulics and segregation. Episodic cascades of particles with processes of shearing and kinematic sieving resulted in coarse materials deposited at the toe of the foreset and medium and coarse sized particles in the mid and upper portion of this slope. The BBW region was dominated by turbidity currents and particles settling after the experiments were complete.

**TSRU tailings BAW has a low slope and a small percentage of the deposit contributed by topset deposition -** Slopes measured in the experiment were similar to those measured in the field ranging between 0.7% and 0.9%. Slope decreased with increasing discharge however flow depth increased.

**TSRU BAW/BBW Transition or foreset is a region of dramatic change in hydraulics and segregation and solids deposition at this location is responsible for a substantial percentage of the BAW -** The experiments suggest that a substantial portion of the BAW deposit is formed through deposition at the foreset including the coarse and heaviest material in the tailings.

**TSRU tailing BBW solids transport is heavily influenced by turbidity currents, which serve to pull coarse material off the BAW and foreset and also allow fines to move farther into the pond -** Thick BBW deposits were generated in the experiments. BBW deposits became part of the BAW deposit as the beach advanced into the pond and therefore constituted a substantial portion of the volume of the BAW deposit.

**TSRU tailings plunge-pool inlet generate large surface froth "islands" that served to segregate fines out of the mixture and store it on the BAW surface -** A surprising observation was the persistent formation of a thick froth at the inlet to the experiment. Analysis of the froth indicates the froth was composed of the finest solids in the tailings mixture and that the fraction of fines captured in the froth is correlated with the inflow discharge rate and plunge pool energy.

**The experiments were success in providing insight into the physics of TSRU tailings disposal and demonstrates the usefulness of lab-based studies.**

## Recommendations

The following recommendation are suggested based on the findings of this research:

1. The generation of surface froth on the BAW is indication of fines segregation. **We suggest that by actually promoting froth formation and capturing this within the BAW region it is possible to reduce the introduction of fines to the pond.**

2. The inflow rate of the TSRU tailings directly affects the flow velocities and bed shear stress in the BAW and thus BBW. The data suggest lower flow rates were associated with better retention of fines in the BAW. High flow rates and higher suspended sediment concentration will also result in more robust turbidity currents capable and greater movement of solids farther into the pond and associated downstream fining segregation processes. **We recommend TSRU tailings discharge be operated at as low a discharge as operationally possible.** For example, continuous discharge at low rates is preferred to higher, intermittent periodic discharge.

3. The surrogate tests, which included a larger fraction of coarser material compared with the TSRU tailings suggests that the presence of coarse material in the tailings stream results in a higher fraction of solids captures on the BAW as well as reduction in the BBW deposit. **We recommend exploring introduction of sand or other coarse material into the TSRU tailings stream or co-deposition of TSRU tailings with a coarser tailings material to improve BAW solids capture.**

4. **We recommend that TSRU tailings research continue to use laboratory-based approaches.** Future research should examine the role of temperature on TSRU tailings transport, segregation and deposition. Research should also examine the opportunity of co-deposition of TSRU tailings with a coarser tailings stream.

## References

Beier, N., Wilson, W., Dunmola, A., & Sego, D. (2013). Impact of flocculation-based dewatering on the shear strength of oil sands fine tailings. *Canadian Geotechnical Journal*, *50*(9), 1001-1007.

Xu, Y., Dabros, T., & Kan, J. (2013). Investigation on alternative disposal methods for froth treatment tailings—part 1, disposal without asphaltene recovery. *The Canadian Journal of Chemical Engineering*, *91*(8), 1349-1357

## Appendix A: List of Publications and patent filing/application

A peer-reviewed publication of this work has not been submitted but the authors do intent on developing a journal paper for publication. COSIA/IOSI will be notified accordingly prior to submission.

The research team presented a summary of the project at two IOSI sponsored workshops in November of 2018 and 2019 in Alberta, CA. These presentations were provided to COSIA/IOSI following the events.

A MS Thesis on Phase 1 of this project is in development at the University of Minnesota by R. Widmer (advisor Kimberly Hill).

## Appendix B: Coring Method

A lab-scale piston coring method was developed for this project and was utilized in both Phase 1 and Phase 2. The method for coring involved the following steps:

- Final deposit survey was used to identify the stream-wise location of the nine cores.
- A single core was pushed through the deposit until it reached the aluminum bed of the flume.
- A tight-fighting end-cap was placed over the end of the copper core tube – creating an airtight seal.
- A second end-cap was prepared.
- The core was slowly lifted out of the deposit and, once free of the water surface, the second end cap was placed over the bottom of the core.

Cores were place in a core-holding device, which kept the core in a vertical position and the cores were place in a freezer until they were ready for analysis.

We used nine coring tubes in total, each consisting of a 33 cm-long copper pipe with a diameter of 2.6 cm. To ensure minimal disturbance of the sediment within each of these cores, we closed the downstream end of the flume and flooded the deposit with water to a depth greater than 33 cm. We inserted the core tubes at our chosen locations vertically with delicacy, so that there was minimal disturbance of the relative location of the sediment within the tube (Figure B1). Once each of the coring tubes reached the bottom of the deposit, we placed a tight cap on the top of the submerged coring tube. We then carefully lifted the coring tube from the deposit so that a second tight cap could be placed on the bottom of the coring tube before the tube left the water. With both caps tightly placed, we removed the coring tube from the flume and placed it vertically in a holding container. This process was repeated for all of the coring tubes. After this was completed, the container containing the filled coring tubes was placed in a freezer to solidify the materials inside the tubes so that the cores could be later split.

**Figure B1. Image of coring tube inserted into final deposit.**

Once the cores were completely frozen, we removed the core samples from the coring tubes and photographed them. We then divided each of the core samples into three approximately evenly sized smaller pieces to be photographed again with labels of the locations where they were extracted. We placed the separated core samples into sample bottles labeled with the coring location and the section of the deposit -- bottom, middle, or top (Figure B2).


**Figure B2. Images of extruded, frozen core (left) and sectioned into bottom, middle and top (right).**

## Appendix C: Extended detail on surrogate materials

All experiment from Phase 1 were using one of two mixtures we considered reasonable surrogate mixtures for TSRU tailings based on certain similar measured characteristics. We determined the composition of the surrogates by comparing the behavior of a small sample of TSRU tailings with several mixtures of materials readily available at SAFL. We found the volumetric concentration of water in the TSRU tailings to be 95% and made test surrogate mixtures that were similar. Then we investigated settling behaviors of the TSRU mixtures and potential surrogate mixtures. We discuss the results of these tests in detail the report.

In the end, we found the most suitable mixture consisted of anthracite coal and kaolinite clay in water for Mixture A and a mixture composed of anthracite coal, kaolinite clay, and silica sand in water for Mixture B. We present the grainsize distributions for anthracite coal, kaolinite clay, and silica sand in **Figures** C1-C3 below.

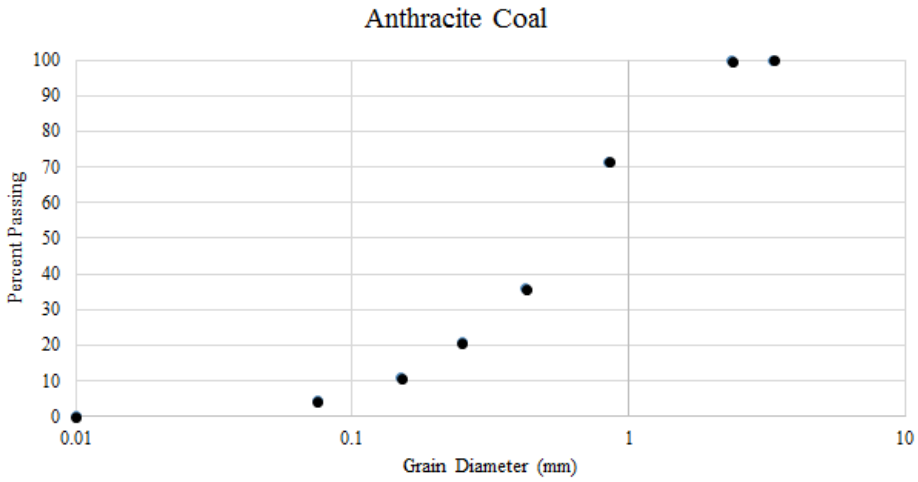


**Figure C1. Grainsize distribution for anthracite coal.**

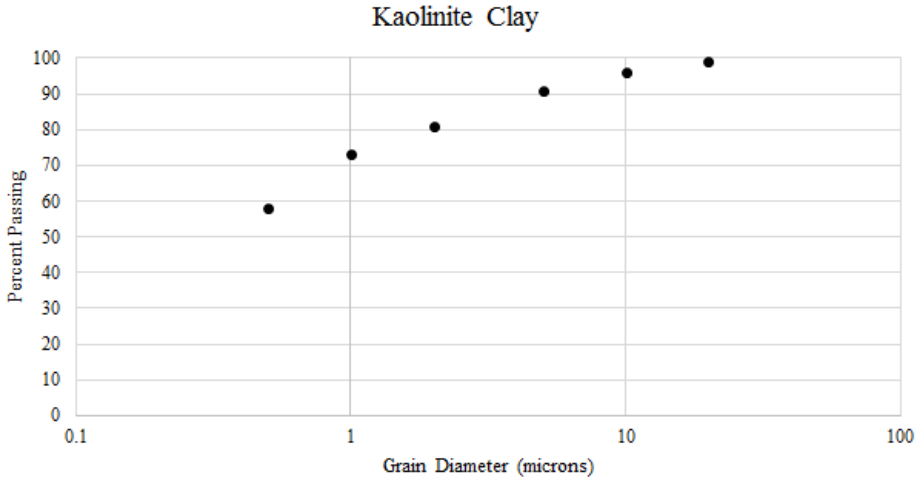


**Figure C2. Grainsize distribution for Snobrite Kaolin clay.**

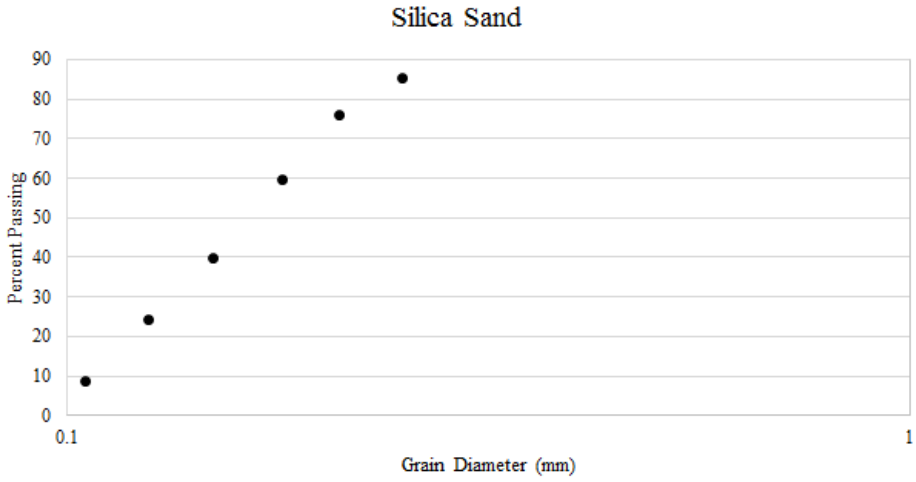


**Figure C3. Grainsize distribution for fine sand.**

We determined the median grain size and other characteristic grain sizes from the Material Safety Data Sheets (MSDS) for the three materials and summarize in Table C1.

**Table C1. Summary of grainsize attributes for the three solids components used to manufacture Surrogate Mixtures A and B.**

| Grain Size (microns) | Anthracite Coal | Kaolinite Clay | Silica Sand |
|---|---|---|---|
| $D_{15}$ | 186 | - | 112 |
| $D_{50}$ | 560 | 0.5 | 164 |
| $D_{85}$ | 1389 | - | 247 |

The experimental parameters for Surrogate Tests 2 and 3 are documented in **Table C2** and in **Table C3** for Surrogate Tests 5 and 6.

**Table C2. Summary of Mixture A recipes used in the Surrogate Tests 2 and 3.**

| | **Experiment** | **Surrogate Test 2** | | **Surrogate Test 3** | |
|---|---|---|---|---|---|
| | **Flow Rate (L/s)** | 0.5 | | 1.0 | |
| **Material** | **Density (g/ml)** | **% Sed. by Vol.** | **% by Vol.** | **% Sed. by Vol.** | **% by Vol.** |
| **Coal** | 1.495 | 89 | 4.5 | 89 | 4.5 |
| **Clay** | 2.82 | 11 | 0.5 | 11 | 0.5 |
| **Silica** | 2.77 | 0 | 0 | 0 | 0 |
| **Water** | 0.9982 | - | 95 | - | 95 |

**Table C3. Summary of Mixture A recipes used in the Surrogate Tests 5 and 6**

| | **Experiment** | **Surrogate Tests 5** | | **Surrogate Tests 6** | |
|---|---|---|---|---|---|
| | **Flow Rate (L/s)** | 1.0 | | 0.5 | |
| **Material** | **Density (g/ml)** | **% Sed. by Vol.** | **% by Vol.** | **% Sed. by Vol.** | **% by Vol.** |
| **Coal** | 1.495 | 44.7 | 2.3 | 44.7 | 2.3 |
| **Clay** | 2.82 | 10.7 | 0.5 | 10.7 | 0.5 |
| **Silica** | 2.77 | 44.7 | 2.3 | 44.7 | 2.3 |
| **Water** | 0.9982 | - | 95 | - | 95 |